

I. Grant Details:

1. Grant Title:	Statewide Wildlife Research
2. SAP/PO (FBMS) #:	F22AF03552
3. Period of Performance (Pop) Start Date:	7/1/2022
4. Period of Performance (Pop) End Date:	6/30/2023

II. Report on Each Objective:

Strategy: Research, Survey, Data Collection, and Analysis

Standard Objective(s): Conduct 12 investigations by 30 June 2023.

Activity(s) Tag/Unit of Measure (with metric): Fish and wildlife species data acquisition and analysis. (12 investigations)

Number of investigations completed 11

Results:

Investigation 1 – Mule Deer Study

Demographics Modeling – We assisted Survey and Inventory project staff with the capture, collaring, and survival monitoring of 304 mule deer (184 6-month-old fawns, four yearling females, 13 yearling males, 46 adult females, and 57 adult males) during winter 2022–2023 for statewide modeling efforts. We used field necropsy techniques to document causes of mortality when possible. We have continued to refine an R Shiny application interface that allows managers and researchers to estimate survival with both Kaplan-Meier and Cox Proportional Hazard models directly from our statewide marked animal database. The application will also allow the estimation of cause-specific mortality with cumulative incidence functions and allow the inclusion of covariates in survival models.

In addition to vegetation growth, snowfall and snow condition have a large influence on mule deer space-use within their winter range. Research collaborators at Colorado State University have produced snow condition estimates across the state of ID from 1995–2019 (SnowModel, Cooperative Institute for Research in the Atmosphere, Colorado State University). This database is at a 90-m spatial resolution and daily time increment. It increases the spatial accuracy by nearly two orders of magnitude relative to previously available snow data (i.e., SNODAS), which is initially provided at a 1-km resolution. Within the past year, we have helped secure funding and a doctoral NSF grant to continue to develop SnowModel, update the model for more recent years, and continue to understand the influence of snow on mule deer survival.

Estimating Habitat Quality – We continued to focus on development and validation of our statewide fine-scale vegetation model. We have funded two M.S. students at the University of

Idaho to lead this effort in conjunction with agency staff. Proposal development for these projects is currently on-going, but a great deal of emphasis will be placed on translating predictions of plant occurrence to measures of nutritional value across the landscape. In summer 2023, the students collected additional vegetation data, focusing on disturbed landscapes to fill in a gap in our understanding of how wildfire influences vegetation communities. The students conducted 194 50-m transects across game management units (GMUs) 1, 6, and 10A. Along these transects, observations of plant species were recorded every m. These observations have been incorporated into our long-term vegetation dataset, landscape covariates were updated in our predictive models, and all models were rerun in preparation for predicting vegetation communities, validating the model, and translating the models into a landscape-scale wildlife nutrition layer.

Estimating Phenological Variation in Nutrition – We have updated the existing Normalized Difference Vegetation Index (NDVI) to December 31, 2021 via a contract with terraPulse (<http://www.terrapulse.com>), providing IDFG with a continuous 30-m spatial resolution of daily NDVI values across Idaho. Annual phenological statistics were also generated providing a data-stream from 2002–2021. Agriculture coverage, forest age, forest extent layers were also extended across the 2019–2021 timeframe.

Regarding other covariates relating to the mule deer nutritional landscape, we reclassified the 2020 USDA-USGS LANDFIRE Existing Vegetation Type (EVT) to create 19 vegetation classes pertinent to ungulate forage. These vegetation classes are a major component of our mule deer winter range models (see section *Seasonal Range and Migration Modeling*).

Integrated Population Models – We have continued work with SpeedGoat (www.speedgoat.io) to refine the mule deer integrated population model (IPM) models and the PopR web interface where they are housed in order to make them more useful and user friendly for agency personnel. Our mule deer IPM provides predictions of demographic parameters at 17 data analysis units (DAUs). We adapted the original IPM to incorporate age-at-harvest data through the addition of population reconstruction. By incorporating this additional data source (age-at-harvest), it has improved our ability to estimate demographic rates and predict population trajectories in DAUs where we have less data on survival, buck:doe ratios, and abundance. We also incorporated all data from this year's mule deer captures and the corresponding survival estimates (see *Demographics modeling*) into the IPM. We have yet to fully implement weather covariates into the IPM pipeline as a means to predict population trajectories in the absence of collaring animals.

Alternative Monitoring Methods – We continued to develop camera-based abundance methods for multiple species, including mule deer. In fall 2022, we revisited and serviced (i.e., replaced batteries and SD cards, replaced damaged/stolen cameras, and re-positioned cameras as needed) most of the 750 cameras that were previously deployed throughout GMUs 1, 6 and 10A. We

reprogrammed randomly placed cameras to begin taking motion- and time-triggered images (at a 10-minute interval) in May 2023, while we reprogrammed trail and road cameras to take motion-triggered pictures only year-round. Cameras not visited during fall 2022 were visited spring 2023 and set to take motion- and time-triggered images. These camera deployments were designed to seasonally estimate the density and abundance of all large mammals, including mule deer, with the methods described by Moeller et al. (2018). Results from the 2021 deployment were reported previously. We processed all pictures taken during summer 2022 with Microsoft's object detection software (MegaDetector; i.e., detects whether images contain something or are empty) and then trained personnel documented the number and species present in those images that contained objects. We have not completed the analyses for the 2022 camera deployment and SD cards from the 2023 deployment are being collected fall 2023.

We are also actively developing methods for estimating fawn:adult doe and adult buck:adult doe ratios using images from trail cameras (Figure 1). In cooperation with Survey and Inventory project staff, we estimated ratios for camera deployments in several areas using cameras deployed in one of three ways, completely random, placed on a dirt-bottomed trail or road nearest a randomly selected location, or placed along a known migration route. Using cameras to estimate ratios remains under development as we explore the influences of seasonal changes in animal movement and differential use of trails and roads dependent upon sex and reproductive status.

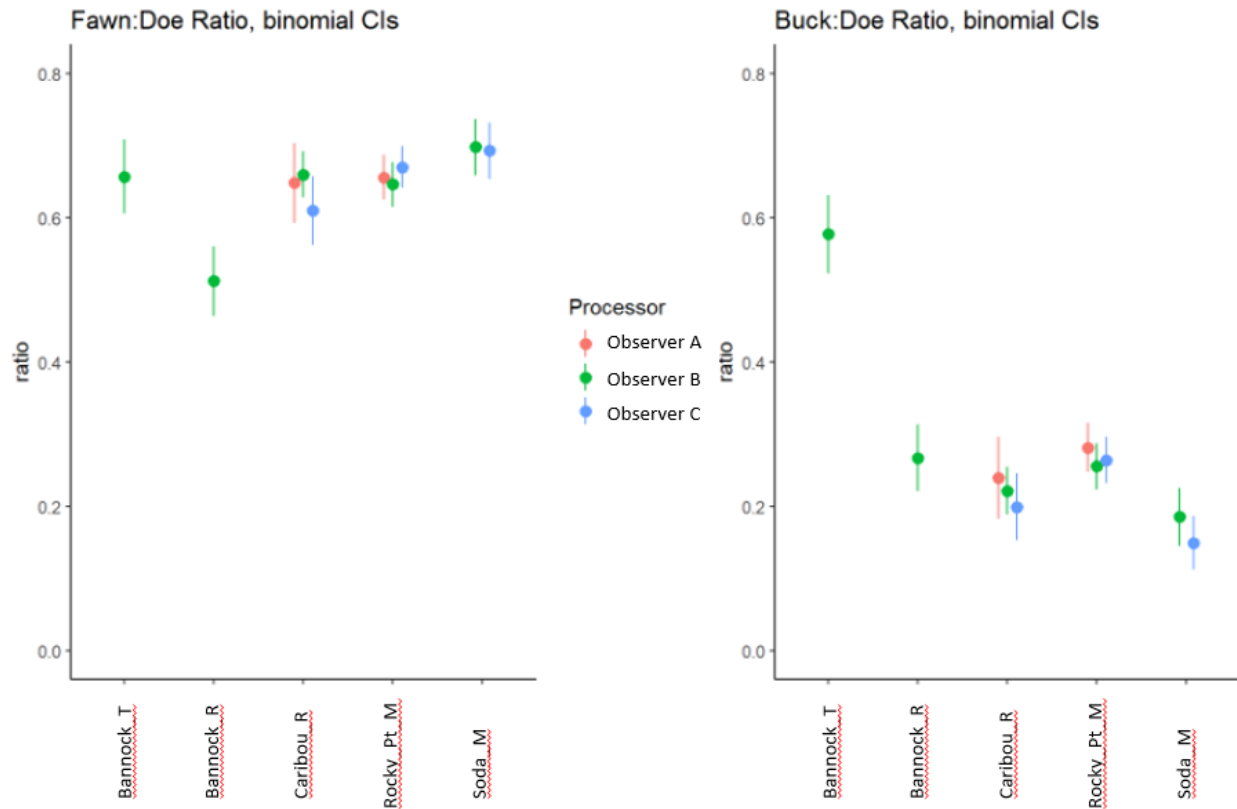


Figure 1. Fawn:Doe (adult female) and Buck:Doe mule deer ratios, with 95% confidence intervals, estimated using images from cameras located on trails and roads (T) or randomly deployed (R) in the Bannock area, randomly deployed (R) in the Caribou area, deployed along a migration route (M) near Rocky Point (PT), and deployed along a migration route (M) near Soda Springs.

Seasonal Range and Migration Modeling – We developed a winter range modeling approach to estimate winter ranges for mule deer across 12 DAUs in southern Idaho. Each of the 12 DAUs is a unique area that uses location and covariate data that are significant and unique to the movement and selection of mule deer within. This methodology used DAU-specific data on the movement metrics, landscape composition, and temporal specificity of seasonally changing covariates (e.g., NDVI and snow conditions) (Table 1). The technique incorporated annually varying data and annually non-varying data (e.g., topographical layers) in a machine learning framework (i.e., random forest) to model and predict winter range use.

Within the winter range modeling framework, there are a series of steps that were used to tailor the methodology to better estimate mule deer winter range within each specific DAU (Figure 2). In the initial step, individual mule deer location data were evaluated using net-squared displacement (NSD; Bunnefield et al. 2011) to determine when the individual was within its winter range (as opposed to more ambiguous date selection techniques). Only winter range locations were used, and non-migratory resident individuals were excluded. For each migratory individual, one winter range location was randomly selected for each day and used in

downstream analyses. Next, available locations were randomly generated within each DAU at a 1 use location:1 available location ratio or a density of ~ 1 location/km², depending upon whether or not the number of use locations within a DAU exceeded the 1 location/km² threshold. Use locations were used to calculate daily movement distances for each individual and then used to identify a mean movement distance across individuals for each DAU. Use and available locations were split into an approximate 70:30 training versus validation structure to be used to calculate area under the receiver operating characteristic curve (AUC) scores for model selection and validation. The daily movement metrics were, in turn, used to buffer each use and available location from the training set. The resulting polygons were used to calculate individual proportions for each of the 19 unique vegetation classes. Additional NDVI, snow covariates, and topographical covariates were attributed for each use and available location. The attributed use and available locations from the training set were then used to build random forest models for each DAU. We used recursive feature elimination to reduce the number of covariates (i.e., identify the optimal model) in each model based upon the highest AUC score (i.e., predictive accuracy) (Figure 3). Variable importance estimation and covariate response curves were generated to better understand the relative influence of covariates on the selection by mule deer for winter range (Figure 4 and 5). The optimal models for each DAU were then used to predict mule deer winter ranges (e.g., Figure 6) across southern Idaho (Figure 7).

We have also estimated and delineated five additional mule deer migration routes, southeastern Idaho, North Hansel Mountains, Albion Mountains, Sand Creek, Southern Hills, and Stone Hills. These databases have been added to IDFG's existing ungulate migration database and published in USGS's Ungulate Migration of the Western United States, Volume 3 (Kauffman et al. 2022).

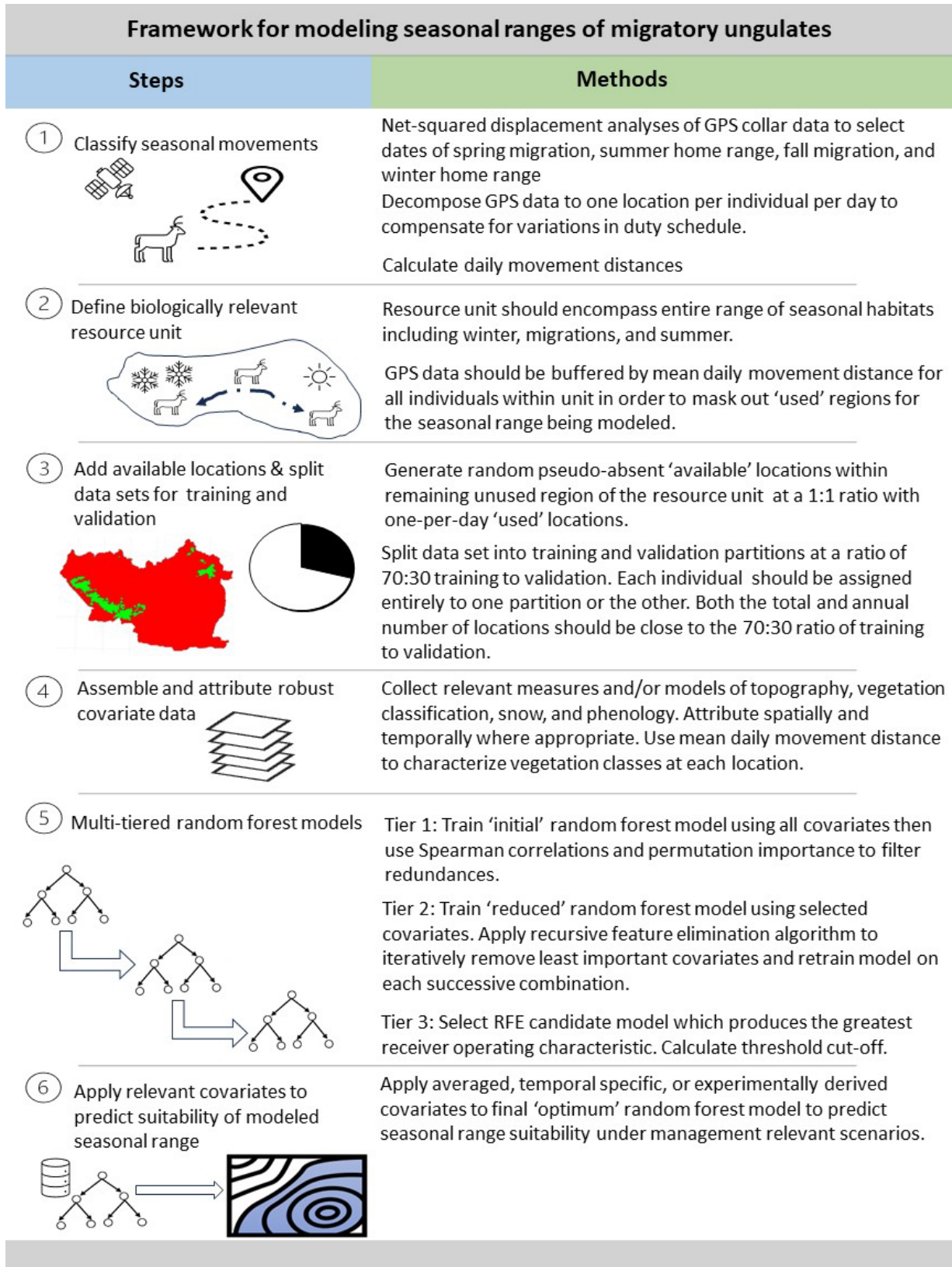


Figure 2. Schematic framework of the winter range estimation methodology for mule deer, elk, and pronghorn antelope.

Table 1. Landscape covariates for Idaho’s big game winter range models.

Type	Covariate	Units	Notes ¹	Species ²
Topography	Aspect	Degrees	0–360 degrees	M, E, P
	Degrees from South	Degrees	0–180 degrees ³	M, E, P
	Degrees from Southwest	Degrees	0–180 degrees ⁴	M, E, P
	Geographic Curvature	Index	500m moving window	M, E, P
	Terrain Ruggedness Index	Index	150m moving window	M, E, P
	Topographic Position Index	Index	500m moving window	M, E, P
	Vector Ruggedness Measure	Index	150m moving window	M, E, P
Snow ⁵	Duration of cover	Days	1999–2019 (Sep 1-Aug 31)	M, E, P
	Median depth	Meters	1999–2019 (Sep 1-Aug 31)	M, E, P
	Maximum depth	Meters	1999–2019 (Sep 1-Aug 31)	M, E, P
Time-Integrated NDVI	Annual	Index	2000–2019 (Jan 1-Dec 31)	M, E, P
	20-year average	Index	2000–2019 (Jan 1-Dec 31)	M, E, P
	20-year median	Index	2000–2019 (Jan 1-Dec 31)	M, E, P
	20-year standard deviation	Index	2000–2019 (Jan 1-Dec 31)	M, E, P
Vegetation Class ⁶	Agriculture	Sq. meters	2001, 2008, 2010, 2012, 2014, 2016	M, E, P
	Aspen	Sq. meters	2001, 2008, 2010, 2012, 2014, 2016	E, P
	Deciduous Shrub	Sq. meters	2001, 2008, 2010, 2012, 2014, 2016	P
	Developed	Sq. meters	2001, 2008, 2010, 2012, 2014, 2016	P
	Evergreen Forest	Sq. meters	2001, 2008, 2010, 2012, 2014, 2016	M, E, P
	Forest (Composite)	Sq. meters	Sum of Aspen, ODF, and EVG	E
	Grassland (Composite)	Sq. meters	Sum of Mesic and Xeric Grassland	M, E, P
	Invasive Grassland	Sq. meters	2001, 2008, 2010, 2012, 2014, 2016	M, E, P
	Juniper Woodland	Sq. meters	2001, 2008, 2010, 2012, 2014, 2016	M, E, P
	Mesic Grassland	Sq. meters	2001, 2008, 2010, 2012, 2014, 2016	M, E, P
	Mesic Sagebrush Shrubland	Sq. meters	2001, 2008, 2010, 2012, 2014, 2016	M, E, P
	Mountain Mahogany Woodland	Sq. meters	2001, 2008, 2010, 2012, 2014, 2016	E, P
	Other Deciduous Forest	Sq. meters	2001, 2008, 2010, 2012, 2014, 2016	E, P
	Riparian	Sq. meters	2001, 2008, 2010, 2012, 2014, 2016	M, E, P
	Sagebrush Shrubland (Composite)	Sq. meters	Sum of Mesic and Xeric Sagebrush	M, E, P
	Unavailable ⁷	Sq. meters	2001, 2008, 2010, 2012, 2014, 2016	P
	Water	Sq. meters	2001, 2008, 2010, 2012, 2014, 2016	P
	Wet Meadow	Sq. meters	2001, 2008, 2010, 2012, 2014, 2016	P
Xeric Grassland	Sq. meters	2001, 2008, 2010, 2012, 2014, 2016	M, E, P	
Xeric Sagebrush Shrubland	Sq. meters	2001, 2008, 2010, 2012, 2014, 2016	M, E, P	

¹All covariate rasters are at a 30-meter resolution

²“M” indicates mule deer, “E” indicates elk, and “P” indicates pronghorn

³0 degrees transformed to be due south (180-degree aspect) and 180 degrees transformed to be due north (0 & 360 degrees). Equation: $Abs(180-Abs(aspect + (180 - 180)))$

⁴0 degrees transformed to be due southwest (225-degree aspect) and 180 degrees transformed to be due northeast (45 degrees). Equation: $Abs(180-Abs(aspect + (180 - 225)))$

⁵Snow covariates were derived from daily estimates of snow cover following the methods of Reinking et al. (2022) and Liston et al. (2020).

⁶Vegetation classes are all measured in scalar square meters

⁷The unavailable vegetation class corresponds well with bare rock lava fields which we expect are strongly avoided by pronghorn

Model Selection (Recursive Feature Elimination)

The Recursive Feature Elimination algorithm selected an optimal model containing 10 covariates.

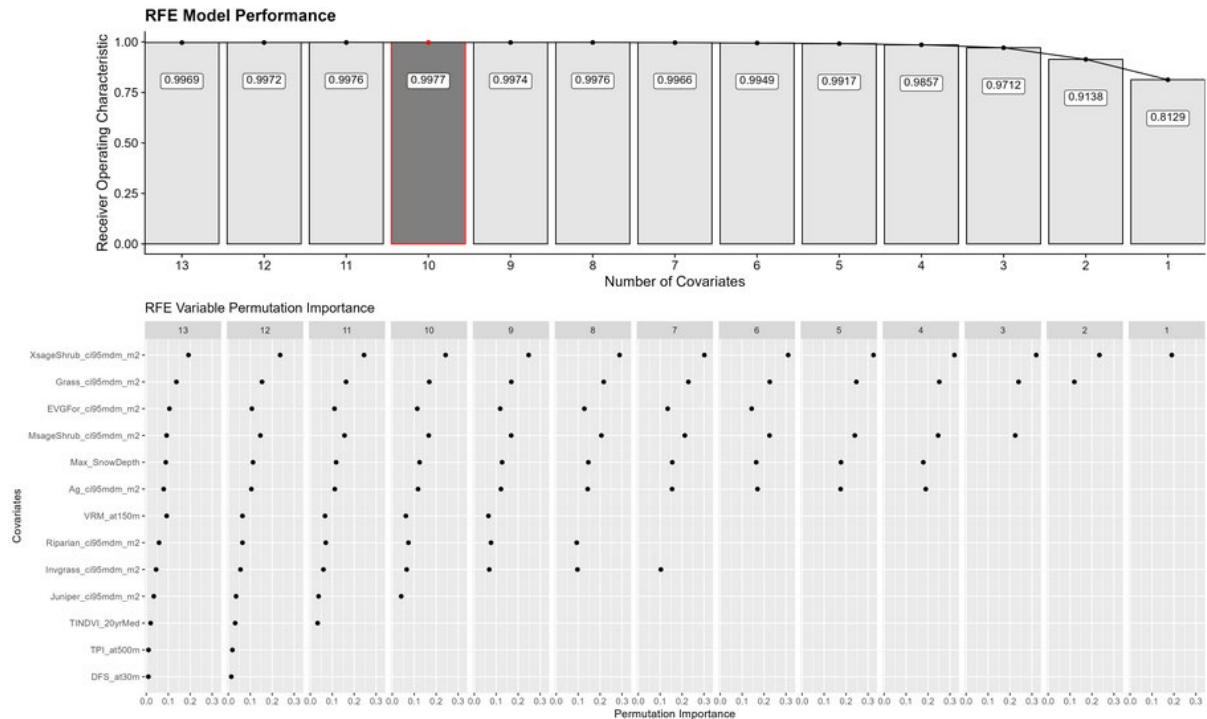


Figure 3. An example of recursive feature elimination (RFE) for a random forest model used to predict mule deer winter range, where the optimal number of covariates is selected based on the highest area under the receiver operating characteristic curve. Within this example, 10 covariates were found to have the highest area under the curve score for the Smokey-Boise DAU winter range model.

Variable Importance Plot

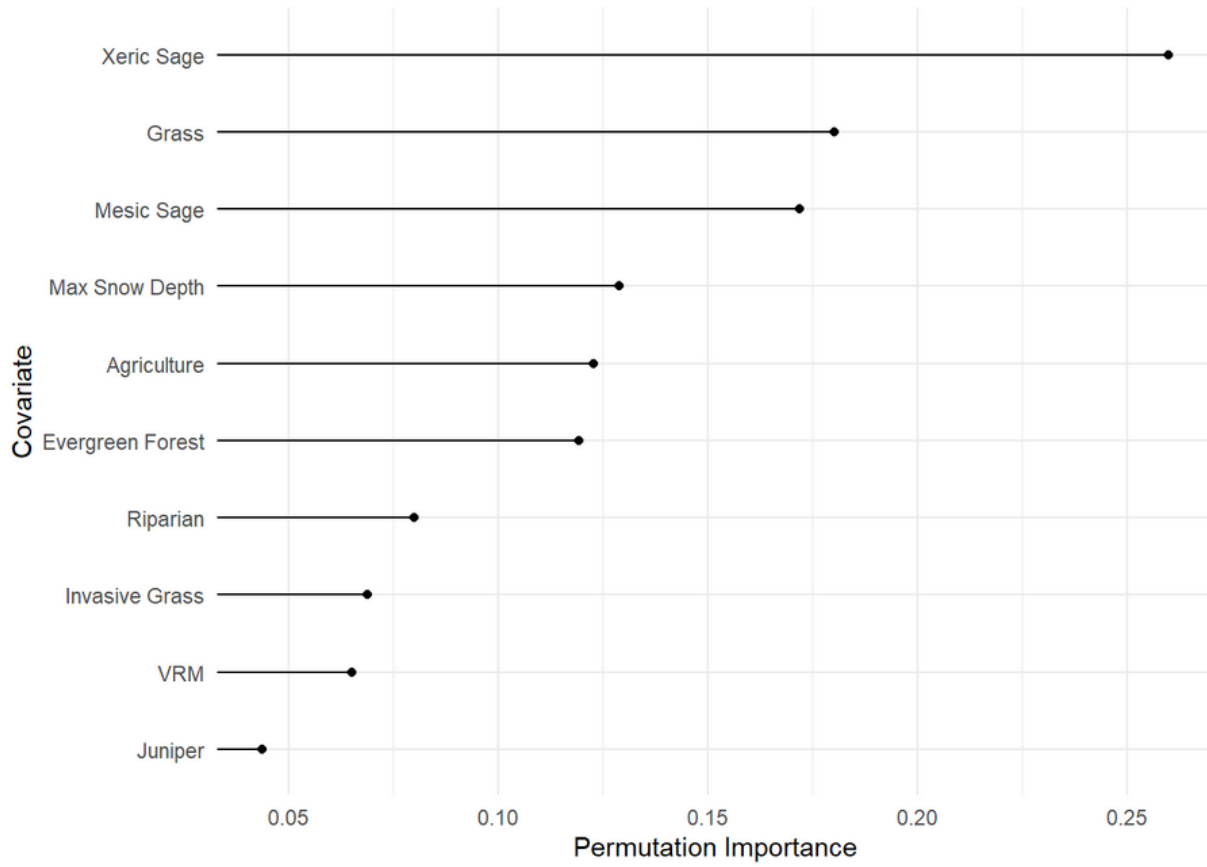


Figure 4. Variable importance of covariates in a random forest model predicting mule deer winter range for the Smokey-Boise DAU.

Covariate Response Plots

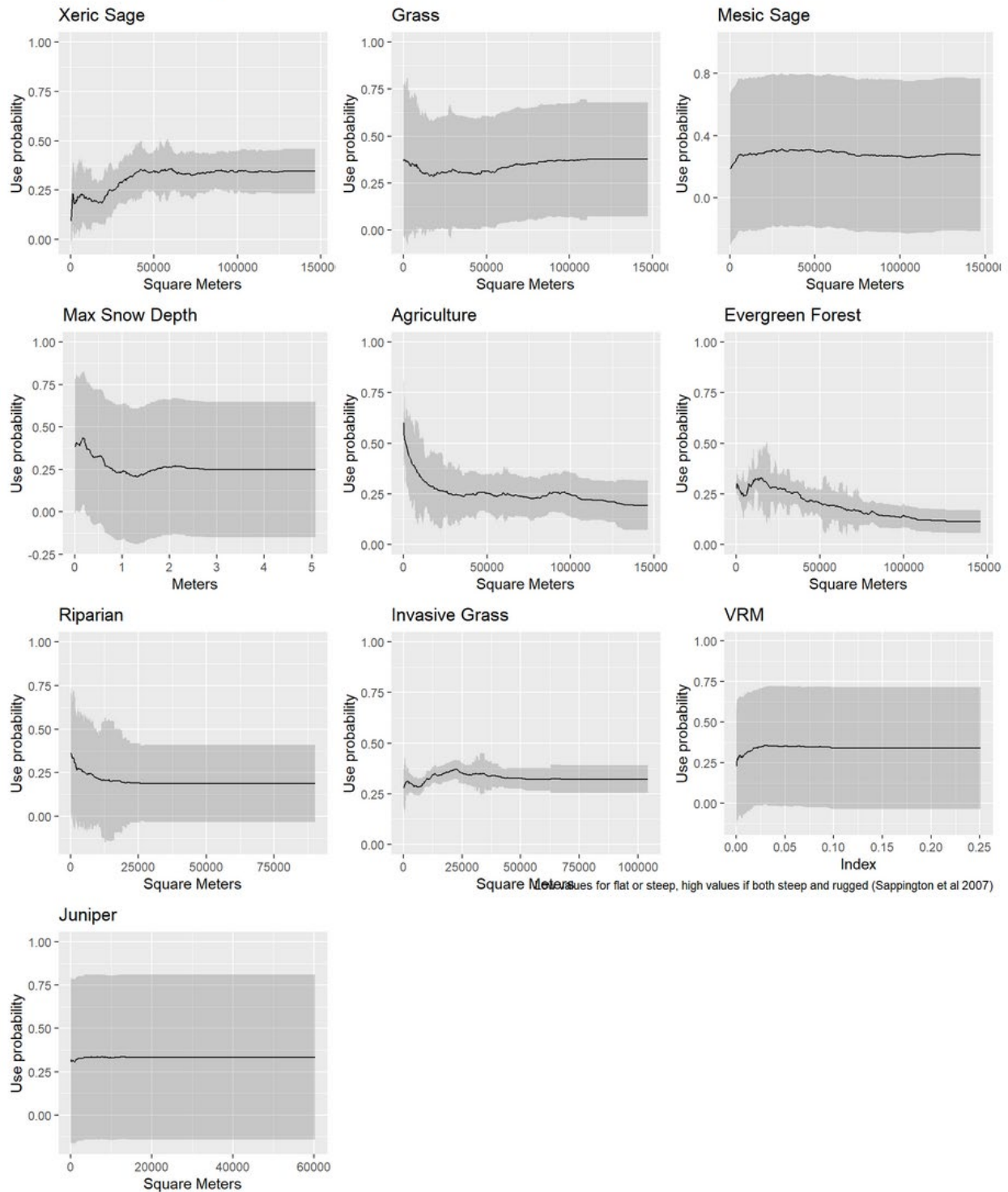


Figure 5. Covariate response curves for covariates in a random forest model predicting mule deer winter range for the Smokey-Boise DAU.

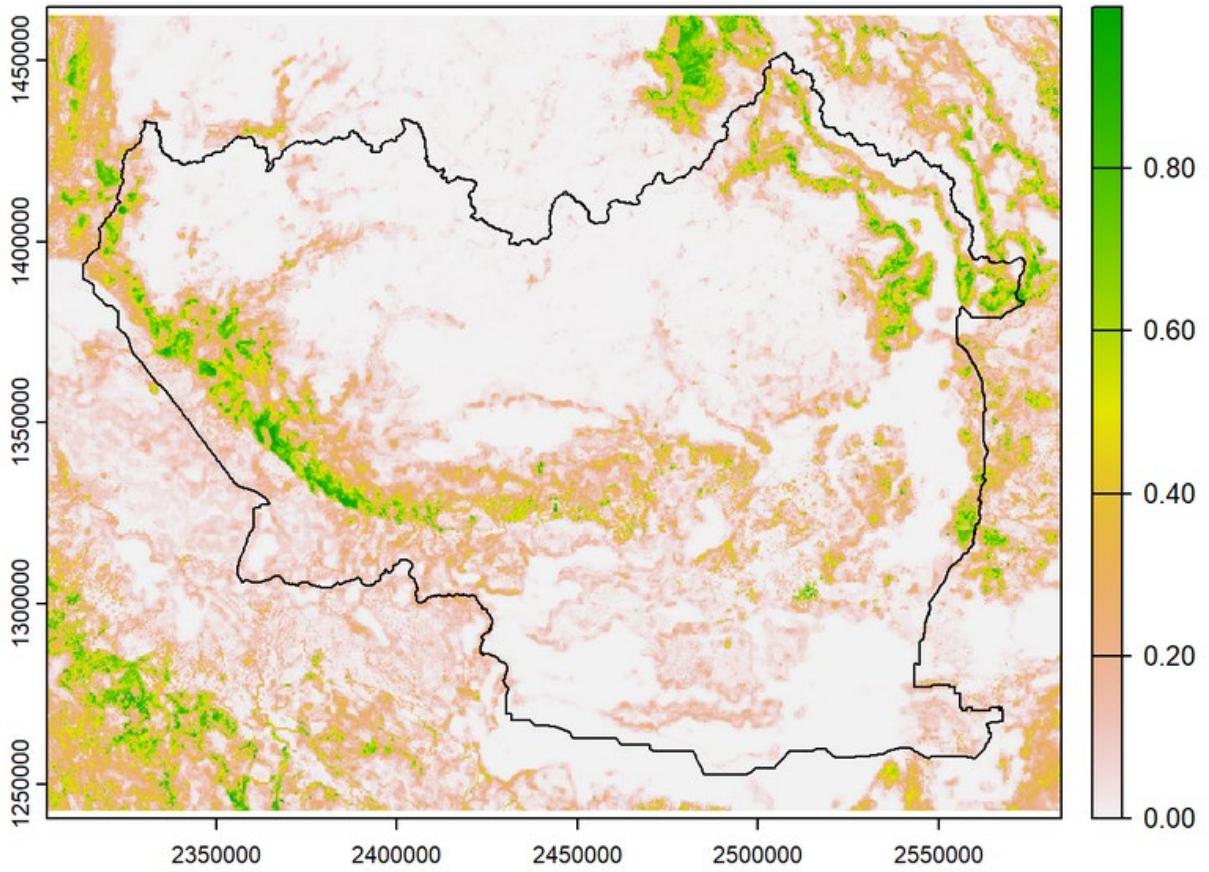


Figure 6. Estimated mule deer winter range for the Smokey-Boise DAU using average snow conditions and 2020 vegetation classes. Green colors represent areas of higher likelihood of use.

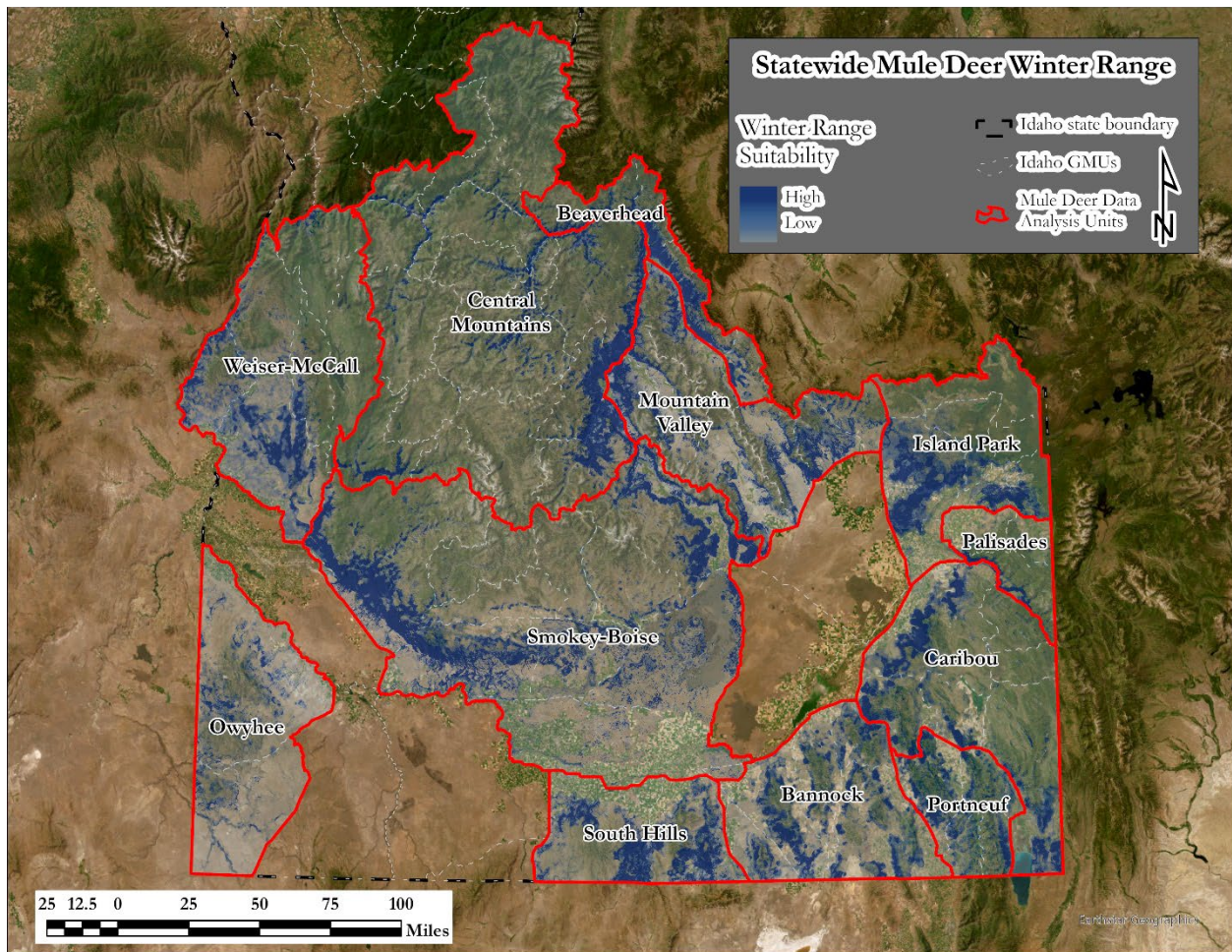


Figure 7. Twelve mule deer winter range estimates for mule deer DAUs occurring in southern Idaho.

Habitat Change and Connectivity Modeling – We continue to use mule deer locations, movements, and seasonal range and migration work to evaluate connectivity and the effects of habitat change. To do so, we are continuing to update the NSD analysis of mule deer using 2022 location data. In conducting this task, we have documented a new movement strategy exhibited by some mule deer in southern Idaho, hereafter deemed winter movement. We have characterized a winter movement as a multiday event, after the end of fall migration and prior to the onset of spring migration, during which an individual moves >10 miles in at least one 24-hour window. We surmise that mule deer are making these movements for the purposes of escaping or mitigating weather events associated with winter severity. Considering that there is higher adult and subadult deer mortality during winter, determining the likely climatic factors that precipitate winter movements will help us better understand the complexity of mule deer spatial responses to winter weather and the downstream demographic consequences.

We have observed ~25% of collared individuals exhibit winter movements within the Owinza mule deer herd. These individuals stop their fall migration in the Picabo Hills, and then, in late winter, move further to the south (on average 35 miles, Table 2). We incorporated these winter movements into the migration analysis for the the Owinza mule deer herd (Figure 8). These winter movements have also been identified in other Idaho mule deer herds (North Hansel and Stone Hills) and Pronghorn Antelope (Gooding and Upper Snake River Plain). Conserving these winter movements are important and have been recognized within Great Basin mule deer herds (van de Kerk et al. 2021). The Owinza mule deer migration route has been incorporated into IDFG's ungulate migration database.

We have had our research on mule deer migrations published in a book with a chapter on mule deer ecology in North America (Kauffman *et al.* 2023). A previous manuscript addressing the use of forced motion variance in the use of delineating and estimating mule deer and elk migrations will submitted for publication during the next reporting period.

We also have developed and evaluated a new method for identifying stopovers that ungulates use along migration routes. Stopovers are often viewed as areas where individuals will rest and forage between faster movement rate transition corridors within a migration route but are often characterized on the landscape as those areas with the highest spatial overlap among migrating individuals. Using collared individuals with a <8-hour fix interval, we first characterized the distribution of migration movement rates. We then calculated the 10% centile of movement rates to establish a threshold under which we considered an individual to be moving slowly (i.e., evidence of a stopover). Our slow movement rate threshold was 2.99 m/minute. For duration, we chose to have individuals maintain this slow rate of movement over a minimum of 12 continuous hours. Following earlier work (Sawyer and Kauffman 2011), we compared stopover estimates at an individual and a population level. Using our approach at the individual level across six mule deer herds, we identified all, but one of the areas identified (18% false positives) as a stopover

using the methods of Sawyer and Kauffman (2011) but found a large number of unique areas (78% false negative) that were not identified as stopovers by the earlier methods. At a population level, we found 54% false positive rate and 41% false negative rate. These differences are quite large and suggest that established methods for identify stopovers in ungulate migration routes might be missing or incorrectly classifying stopovers. The analyses identifying mule deer, elk, and pronghorn stopovers are being prepared for publication as a peer-reviewed manuscript.

Finally, we conducted an exploratory study to investigate whether the sequence of poor forage quality summers followed by severe winters is increasing or decreasing across 18 winter mule deer herds in southern Idaho. Poor summer vegetation production can yield lower energy storage reserves in individuals (e.g., fat reserves). These energy reserves are needed by the individual to survive food limited winter conditions where these energy reserves are drawn upon. The sequence of below average vegetation production and severe winters might cause reduced physiological condition population-wide, leading to reduced survival and reproduction. To better understand occurrences of poor summer conditions followed by severe winter conditions, we estimated utilization distributions (UDs) to approximate mule deer summer and winter ranges. Within UD, annual TNDVI was estimated across an 18-year timespan (2002–2019) and used as an index of vegetation growth and summer conditions. We then calculated the mean and interquartile range of TNDVI across years to establish average summer conditions. We took a similar approach to maximum snow depth. Each year was given a summer condition score dependent upon whether it was below the mean (1) or below the first quartile (1.5) and a winter condition score dependent upon whether it was above the mean (1) or above the third quartile (1.5). The summer and winter scores were then combined for each year and the trends for summer condition, winter condition, and in combination were evaluated to determine if conditions for each mule deer herd were declining or improving (Table 3).

Table 2. The timing, duration, and distance of mule deer individuals using winter movements between the Picabo Hills to terminal winter range south of Owinza, Idaho.

Animal_ID	Movement Start Date	Movement End Date	# of Days	Distance (km)
19592	1/16/2020	1/21/2020	6	64.95
210200	2/5/2021	2/12/2021	8	74.71
211523	12/27/2021	12/29/2021	3	37.80
220291	1/8/2023	1/13/2023	6	69.50
220294	1/12/2023	1/17/2023	6	39.05
220375	1/11/2023	1/15/23	5	45.67
		average	5.66	55.28

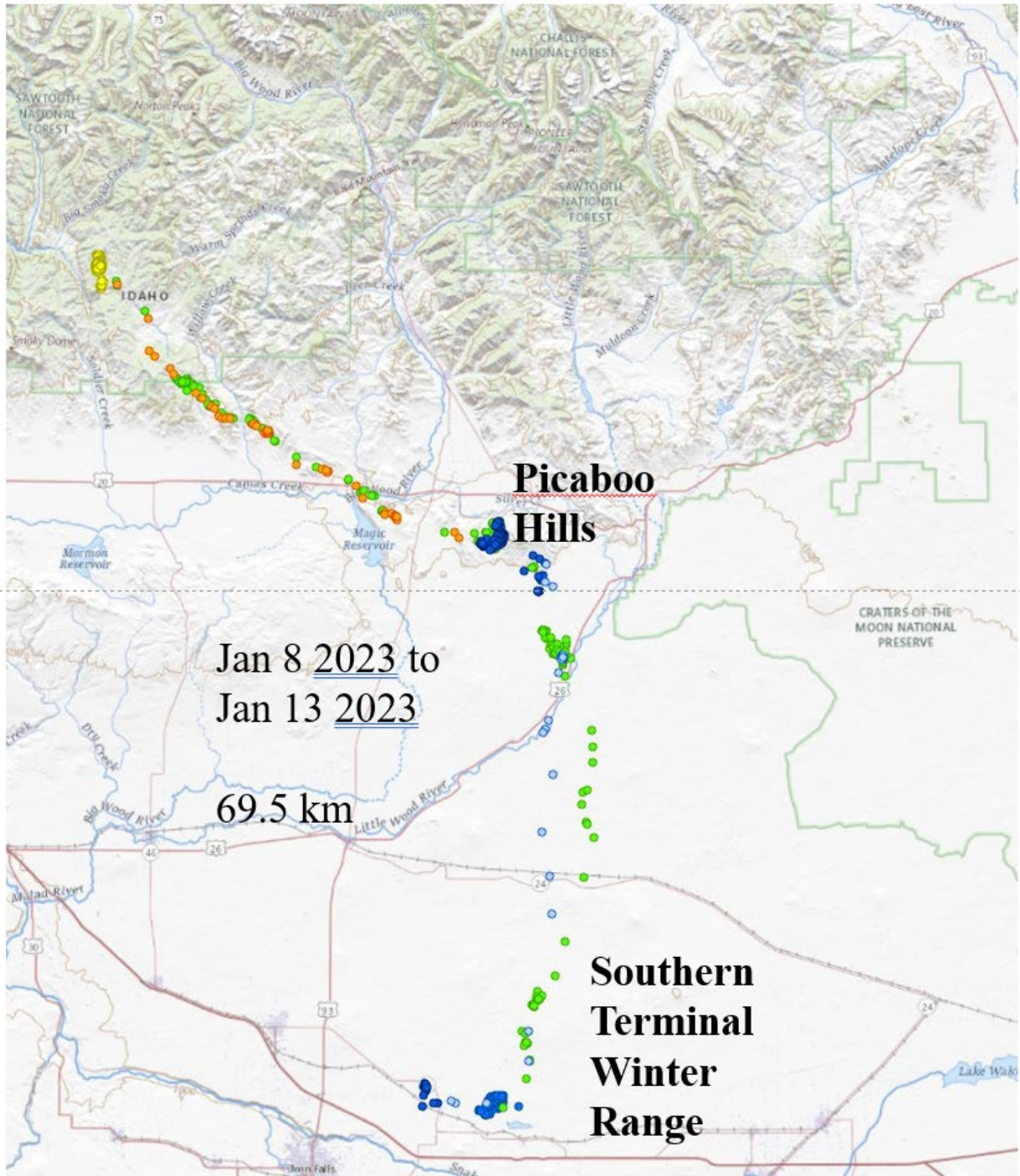


Figure 8. An example of an extended winter movement by an individual of the Owinza mule deer herd in southern Idaho.

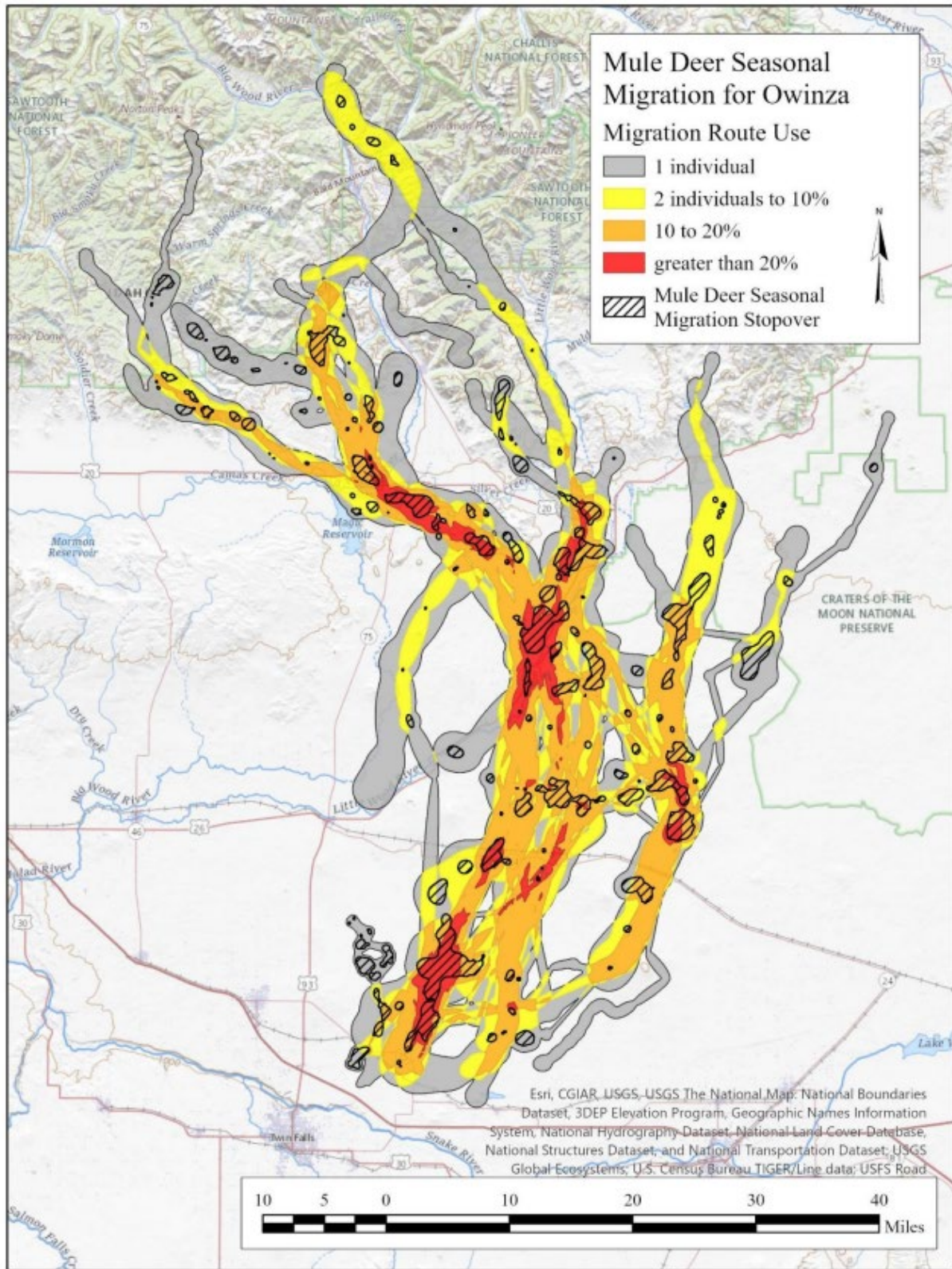


Figure 9. Mule Deer Seasonal Migration Route for the Owinza mule deer herd in southern Idaho.

Table 3. Trajectories of seasonal and sequential below normal forage production, above normal winter snow maximum, and the sequence of the two seasonal conditions through time 2002–2019.

Herd	Vegetation Threat Trajectory	Snow Threat Trajectory	Combination Threat Trajectory
Antelope Creek	decreasing	decreasing	decreasing
Albion Mountains	increasing	increasing	increasing
Blacks Creek	increasing	decreasing	increasing
Bear Lake Plateau	decreasing	increasing	increasing
Bennett - Teapot	decreasing	decreasing	decreasing
Emmitt	increasing	decreasing	decreasing
Morgans Creek	decreasing	increasing	increasing
North Fork Salmon	increasing	increasing	increasing
Palisades	decreasing	decreasing	decreasing
Pioneer Reservoir	decreasing	no change	decreasing
Reese Creek	decreasing	increasing	increasing
Reno	decreasing	decreasing	decreasing
Sand Creek	increasing	decreasing	decreasing
Soda Hills	no change	decreasing	decreasing
South Hills	decreasing	increasing	decreasing
Stone Hills	decreasing	increasing	decreasing
Tex Creek	decreasing	increasing	increasing
Teton River	decreasing	decreasing	decreasing

Buck Vulnerability – We extended the drop off dates for GPS-collared male fawns that were captured as part of the Survey and Inventory project survival monitoring program, allowing us to use those collars as part of the buck vulnerability investigation. During the reporting period, we caught 98 male fawns, 13 yearling males, and 57 adult bucks to investigate buck vulnerability. We caught the adult bucks in GMUs 22, 32, 39, and 40 to evaluate the effect of 2-point only and general hunting seasons on buck vulnerability. We continued efforts to test new technologies that will allow transmitter deployment on bucks of all age classes through the rut. We deployed 10 eartag units equipped with GPS transmitters on adult bucks in GMU 40 during August 2020, all of which failed. We subsequently purchased additional units from 2 different manufacturers and plan to deploy and test them this winter.

We will use deer collared for this project to predict the effects of access, hunting season structure, and habitat security on male deer survival. Because one season type or structure will not produce the same mortality results in GMUs with different hunter access and security cover, we plan to alternate through tests of season type and habitat security, while maintaining adequate control over GMUs. This project is utilizing the ongoing statewide vegetation modeling efforts to provide vegetation security cover estimates. We will monitor these individuals, and additional collared male deer in future years, for survival and movements related to habitat and human activity until death or collar failure. This research will provide managers with objective estimates of the effects of changing hunting season structure and habitat security, with the goal of maintaining hunter opportunity. In years 2019–2023, we have documented 112 mortalities of collared adult and yearling male mule deer in GMUs 22, 32, 39, and 40.

Chronic Wasting Disease – Research staff assisted Survey and Inventory project staff in estimating the prevalence and spread of chronic wasting disease in GMU 14. We estimated prevalence rates of 0%, 1.17%, and 7.04% in elk, mule deer, and white-tailed deer, respectively, that were harvested in GMU 14. We did not collar any animals as part of our effort to monitor the spread of CWD.

Investigation 2 – White-tailed Deer Study

No additional white-tailed deer were captured and collared from August 2022–June 2023. We continue to monitor deer captured and affixed with collars in previous years. From August 2022 to June 2023, 20 white-tailed deer died from various causes (Table 4). Only one mortality occurred in 10A (unknown mortality cause). All other mortalities ($n = 19$) occurred in GMUs 1 and 6.

Table 4. Confirmed mortalities of collared white-tailed deer from August 2022–June 2023. Number and sex of deer (M=male or F=female) are indicated.

Fate	Description	<1 Year	Yearlings	Adults	Total
Non-Predation	Car Strike	1 (1F)	1 (1F)	1 (1F)	3
	Harvest		4 (1M, 3F)	3 (2M,1F)	7
Predation	Mountain Lion	2 (1M,1F)		1 (1F)	3
	Unknown Predation	2 (2M)	1 (1F)		3
Unknown	Unknown Mortality	3 (2M,1F)		1 (1F)	4
Total		8	6	6	20

We continue to monitor 13 white-tailed deer in GMU 1, two white-tailed deer in GMU 6, and two white-tailed deer in GMU 10A (Table 6) with active collars. We also have two mule deer with active collars in GMU 6 that were captured and collared in 2020 and 2021, respectively.

Table 5. Female deer in GMUs 1, 6, and 10A with active collars. Collared deer are white-tailed deer unless indicated otherwise.

Captured	Current Age Class	1	6	10A
Winter 2020	Adult		1 (1 Mule Deer)	2
Winter 2021	Adult	4	2 (1 Mule Deer)	
Winter 2022	Yearling	2	1	
Winter 2022	Adult	7	1	

We also continue to monitor white-tailed deer, and other species, using cameras in GMUs 1, 6, and 10A as detailed in the *Alternative Monitoring Methods* section of the Mule Deer Study. In fall 2022, we visited and serviced (i.e., replaced batteries and SD cards, replaced damaged/stolen cameras, and re-positioned cameras as needed) most of the 750 cameras that were previously deployed throughout GMUs 1, 6 and 10A. We programmed randomly placed cameras to begin taking pictures in May 2023, while we reprogrammed trail and road cameras to take motion-triggered pictures only year-round. We processed all pictures taken during summer 2022 with Microsoft’s object detection software (MegaDetector; i.e., detects whether images contain something or are empty) and then trained personnel documented the number and species present in those images that contained objects. Preliminary summer abundance estimates for white-tailed deer in GMUs 1, 6, and 10A using images collected in summer 2021 were previously reported. Images from summer 2022 are still be processed, and thus newer estimates are not yet available.

Chronic Wasting Disease – See *Chronic Wasting Disease* section under Mule Deer Study

Investigation 3 – Elk Study

Modeled Effects of Predator Harvest on Ungulate Survival – We evaluated the utility of the multi-predator, multi-prey model that was developed as a result of an IDFG-supported PhD project at the University of Montana. In prior reports, the development of the model was detailed, and its use in testing theory has been published elsewhere (Clark et al. 2021). To evaluate the model as a management tool, we simulated theoretical predator-prey communities under a variety of densities and strengths of species interactions. The complexity of predator-prey communities was beyond the ability of the model to accurately capture. Many of the model parameters proved unidentifiable. With a greater understanding of species interactions, it might be possible to improve the model, but the expense and practical constraints of such an undertaking likely make it infeasible to do so.

Elk Population Modeling – We continued the development of a suite of online tools designed to help managers estimate and monitor elk populations and continued our evaluation of several methods for obtaining the vital rate data needed to populate an integrated population model to estimate annual elk abundance throughout Idaho (i.e., periodic population estimates, survival of young, survival of adults, fecundity, and harvest rate).

We contracted with SpeedGoat (www.speedgoat.io) to develop the integrated population model structure and incorporate it into their online modeling and reporting interface, PopR. The online platform was updated throughout the year with many of those updates focused on improving reliability and ease of use. We have added a population reconstruction component to the platform to improve model estimates in areas that have limited data. We assisted Survey & Inventory project staff with placing collars on 16 adult female and 198 6-month-old calf elk of both sexes in 9 areas of the state, which represent the primary ecotypes of the state with replication, to estimate survival. We are using these survival rates to represent the survival of neighboring elk zones with similar ecotype and predator density in the integrated population model.

Seasonal Range and Migration Modeling – We have developed a winter range modeling approach that has been used across six elk zones in Southern Idaho (Figure 10). Each zone is a unique area that uses location and covariate data that are unique to the movement and selection of elk within. This methodology used zone-specific data on the movement metrics, landscape composition, and temporal specificity of seasonally changing covariates (e.g., NDVI and snow conditions) (Table 1). The technique incorporated annually varying data and annually non-varying data (e.g., topographical layers) in a machine learning framework (i.e., random forest) to model and predict winter range use. Details of the modeling approach are presented in the *Seasonal Range and Migration Modeling* section of the Mule Deer Study.

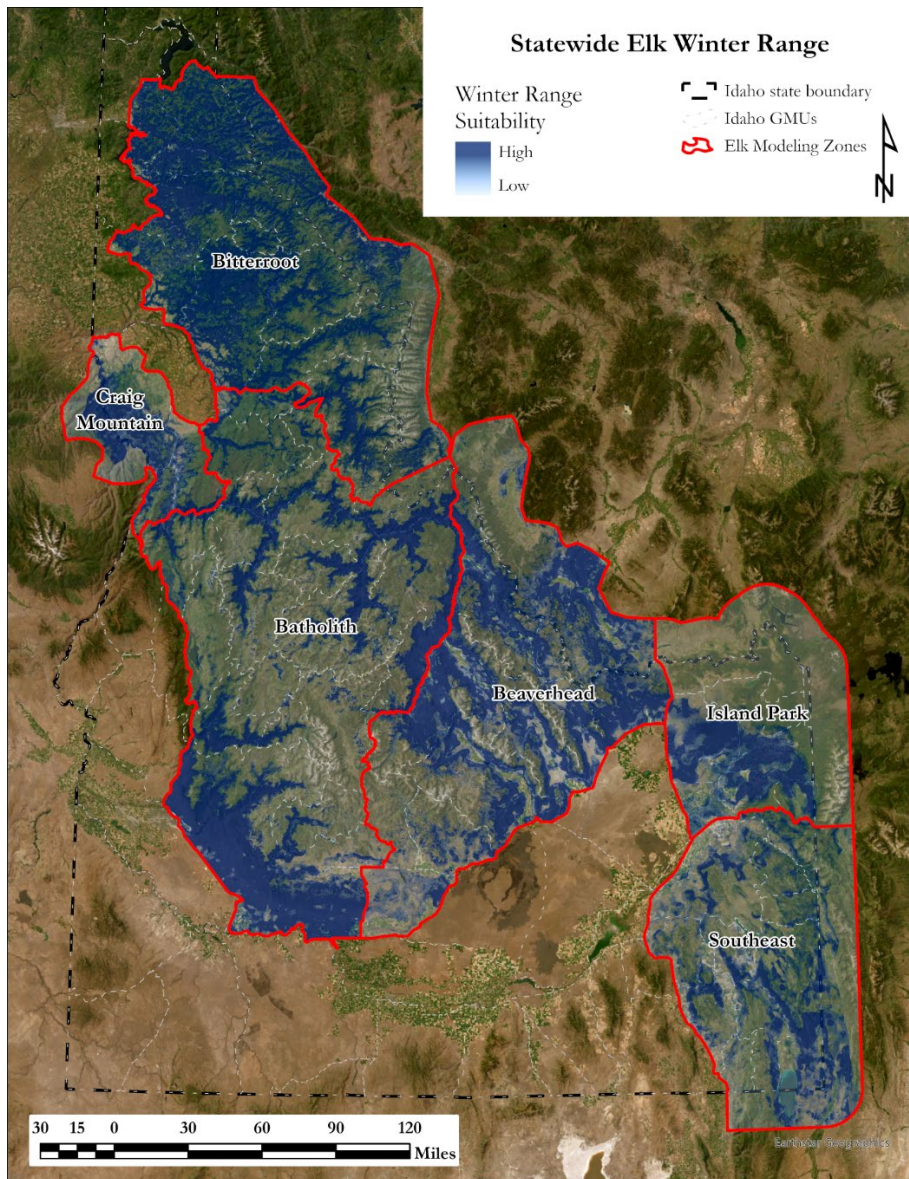


Figure 10. Estimated winter range for elk in six elk zones.

We estimated and mapped seven additional elk migration routes for Idaho, Black Prince-Slate Creek, North fork of the St. Joseph River, Rochat Creek-Ahrs Creek, Sand Creek, South St. Joseph River, Teton River, and Trout Creek-Big Creek. These databases have been added to IDFG’s existing ungulate migration database and published in USGS’s Ungulate Migration of the Western United States, Volume 3 (Kauffman et al. 2022).

We also developed and evaluated a new method for identifying stopovers that ungulates use along migration routes (see the *Seasonal Range and Migration Modeling* section of the Mule Deer Study). For three herds that consisted of 459 tracked migrations of individual collared elk, we found that when compared to the methods proposed by Sawyer and Kauffman (2011), false

positives (identification of different stopovers) were found to occur at a rate of 16%. False negatives (failure to identify stopovers) occurred at a much higher rate of 89%. At the population level, false positives and false negatives occurred at 14% and 65%, respectively. The methods and associated findings were presented at the national TWS conference in Spokane, WA in Nov 2022 and WAFWA Deer and Elk workshop in May of 2023. The analyses identifying mule deer, elk, and pronghorn stopovers are being prepared for publication as a peer-reviewed manuscript.

Alternative Monitoring Methods – We also continue to monitor elk, and other species, using cameras in GMUs 1, 6, and 10A as detailed in the *Alternative Monitoring Methods* section of the Mule Deer Study. In fall 2022, we visited and serviced (i.e., replaced batteries and SD cards, replaced damaged/stolen cameras, and re-positioned cameras as needed) most of the 750 cameras that were previously deployed throughout GMUs 1, 6 and 10A. We programmed randomly placed cameras to begin taking pictures in May 2023, while we reprogrammed trail and road cameras to take motion-triggered pictures only year-round. We processed all pictures taken during summer 2022 with Microsoft’s object detection software (MegaDetector; i.e., detects whether images contain something or are empty) and then trained personnel documented the number and species present in those images that contained objects. Preliminary summer abundance estimates for elk in GMUs 1, 6, and 10A using images collected in summer 2021 were previously reported. Images from summer 2022 are still be processed, and thus newer estimates are not yet available.

In addition to estimating abundance using these cameras, we are also developing methods to estimate elk herd composition (calf:adult cow and adult cow:adult bull ratios). We assessed over 481,000 pictures of elk collected using cameras in GMUs 1, 6, and 10A during summer and winter in 2020 and 2021. We determined that cameras deployed at random locations on roads or trails had a higher proportion of cameras with pictures of elk (80%) versus those cameras deployed at random points (64%). We also found that we captured more images of elk between July and September compared to other months of the year (Figure 11). We observed that estimates of age ratio were relatively similar between cameras placed on roads and trails and cameras placed randomly (Figure 12) but that sex ratios fluctuated depending on camera deployment style (Figure 13).



Figure 11. Total number of elk classified in GMU 1 from June to October in 2021.

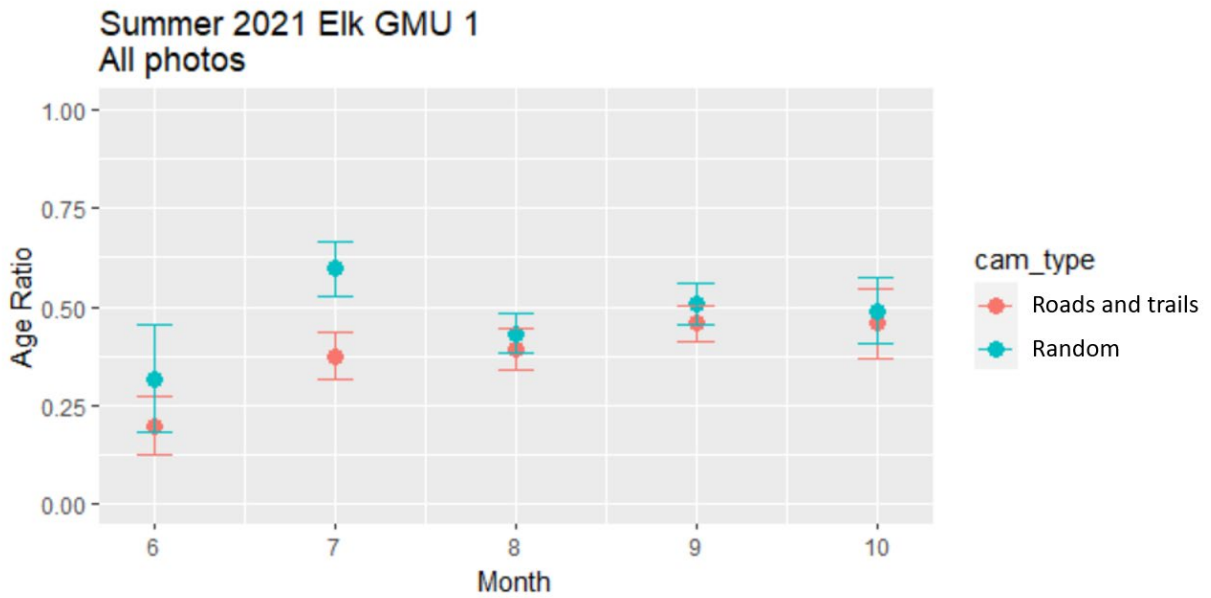


Figure 12. Monthly age ratio estimates in GMU 1 from June to October 2021.

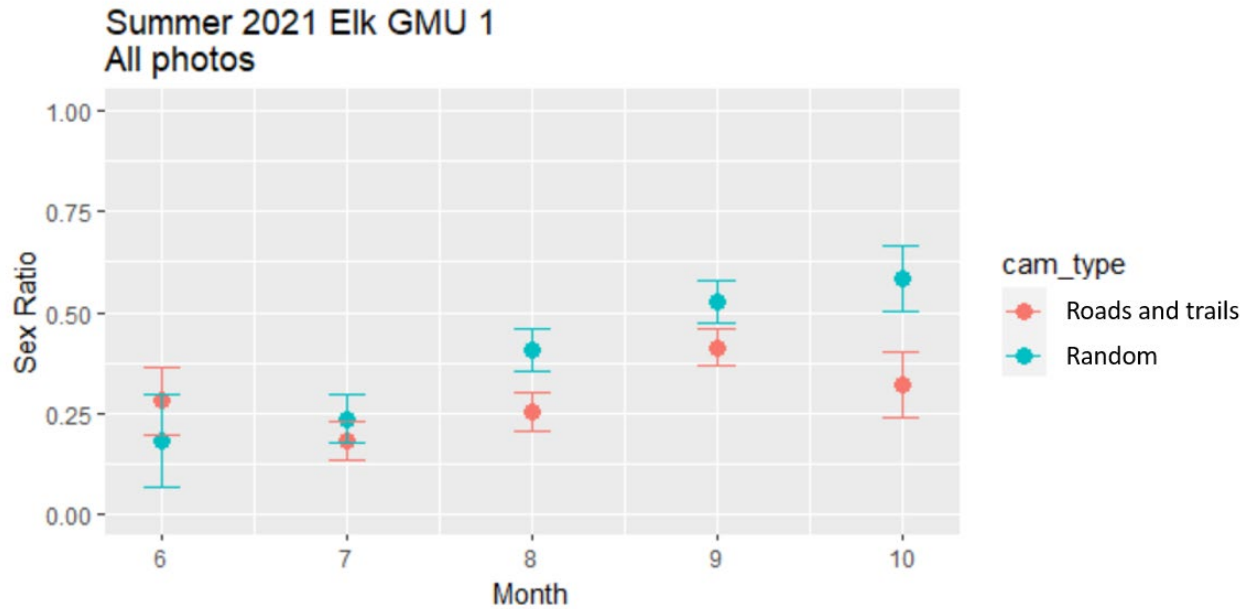


Figure 13. Monthly sex ratio estimates in GMU 1 from June to October 2021.

Similar to mule deer, we also examined the utility of estimating elk herd composition using cameras placed along migration routes. We deployed 20 cameras in the Sawtooth Elk Zone in fall 2021 and 2022. The cameras were placed in clusters along five areas identified within the Sawtooth elk migration route along the South Fork of the Payette River. Cameras were deployed in late October through November and collected in late March. We compared camera-based ratio estimates to ratios from aerial surveys conducted as part of the Survey and Inventory project in the same area in February 2022 and 2023 to determine if this methodology results in similar ratio estimates for elk in the Sawtooth Elk Zone. The age ratio estimate from the 2021 camera array was 27 calves:100 cows and the age ratio estimate from the 2022 aerial survey was 29 calves:100 cows suggesting the estimates from cameras placed on migration routes are similar to those from aerial surveys. Sex ratios were not available from the 2022 aerial survey but the estimated sex ratio from camera data (12 bulls:100 cows) was similar to sex ratios from the 2023 aerial surveys for this elk population (11 bulls:100 cows). We repeated camera deployment in the fall of 2022 and compared results to a more comprehensive aerial survey flown by Survey and Inventory project staff in February 2023. The age ratio estimate from the 2022 camera array was 27 calves:100 cows and the age ratio estimate from the 2023 aerial survey was 32 calves:100 cows. We are continuing work to validate the use of cameras to estimate herd composition and will be deploying cameras on migration routes again in fall 2023 to compare to the February 2024 aerial survey.

Chronic Wasting Disease – See *Chronic Wasting Disease* section under Mule Deer Study

Investigation 4 – Bighorn Sheep Study

Disease Ecology - We captured 188 bighorn sheep August 2022–March 2023. We collected samples at capture to test for exposure to, and carriage of, the respiratory pathogen *Mycoplasma ovipneumoniae* (Movi), other bacteria, parasites, and respiratory viruses and used ultrasound and palpation to estimate body condition (Table 6). All health testing was conducted at the Washington State University Disease and Diagnostic Laboratory (WADDL).

Table 6. Bighorn sheep captures in Hells Canyon, July 2022–March 2023.

Population	Female	Male	Lamb	Total
Asotin	15	4	12	31
Big Canyon	5	5	3	13
Black Butte	6	4	3	13
Imnaha	12	6	5	23
Lostine	5	10	1	16
Lower Hells Canyon	4	0	3	7
Mountain View	8	9	5	22
Redbird	22	12	4	38
Tucannon	1	1	0	2
Wenaha	13	6	4	23
Total	91	57	40	188

We monitored movements, productivity, and survival of 300–353 marked bighorn sheep from the air and ground between May 2022 and April 2023. By the end of the biological year, accounting for sheep entering the study and deaths there were 353 marked sheep in the project area (Table 7).

Table 7. Collared and marked sheep present in Hells Canyon bighorn sheep populations as of April 30, 2023.

Population	Active Collars				Marked Sheep ^a		Total
	M		F		M	F	
	VHF	GPS	VHF	GPS			
Asotin ^b	1	1	2	14	6	16	22
Big Canyon	5	3	7	5	7	12	19
Black Butte	1	4	5	5	8	17	25
Imnaha	0	8	4	14	9	18	27
Lostine	0	9	9	3	16	28	44
Lower HC	1	0	7	6	4	20	24
Mountain View	1	9	14	4	13	25	38
Muir Creek	1	0	2	0	4	4	8
Myers/UHC-ID	0	0	3	0	1	3	4
Redbird	2	12	17	20	26	50	76
Saddle Creek	0	1	1	5	3	8	11
Tucannon	1	0	2	1	3	9	12
Wenaha	3	7	10	13	14	29	43
Total	16	54	83	90	114	239	353

^aIncludes functional collars, non-functional collars, and non-collared, ear-tagged sheep.

^bDoes not include neonate lambs hand captured in the 2022 biological year, see section on lamb capture below.

Field effort for monitoring productivity and lamb survival was reduced in 2022. We observed 85 of 129 marked ewes in eight populations with lambs during the 2022 biological year (Table 8). Of the lambs observed, 61 of 85 (72%) survived over the summer (≥ 1 October). No pneumonia was documented in lambs in the populations monitored. A stillbirth in Asotin Creek discovered as part of the University of Idaho graduate study (see below) was attributed to fetal infection with the parasite *Toxoplasma gondii*. A report led by WADDL on Toxoplasmosis in bighorn lambs describing cases from Asotin Creek, the Bison Range, Montana, and the Wildcat Hills, Nebraska was published in the Journal of Wildlife Diseases (Fisk et al. 2023).

Table 8. Observed productivity of marked ewes and survival of lambs born in 2022 in 12 Hells Canyon bighorn sheep populations.

Population	<i>n</i> marked ewes	<i>n</i> marked ewes w/lambs	October 1 lambs (summer survival)
Asotin	21	17 (81%)	11 (65%)
Black Butte	7	6 (86%)	5 (83%)
Imnaha	12	7 (58%)	6 (86%)
Lower Hells Canyon	14	10 (71%)	5 (71%)
Mountain View	18	10 (55%)	9 (90%)
UHC- Idaho	3	2 (67%)	-
Redbird	39	25 (82%)	21 (84%)
Wenaha	15	5 (56%)	4 (80%)
TOTAL/AVERAGE	129	85(72%)	61 (72%)

Overall, adult survival was high in 2022 (Table 9). Nineteen radio-collared sheep died with causes of death assigned as harvest (6 males), infection or injury ($n = 5$), predation or probable predation ($n = 3$, and unknown causes ($n = 5$).

Table 9. Survival of radio-collared adult bighorn sheep in 13 Hells Canyon populations, May 1, 2022–April 30, 2023.

	Female			Male		
	<i>n</i>	<i>n</i> survived	survival	<i>n</i>	<i>n</i> survived	survival
Asotin	21	18	0.86	3	2	0.67
Big Canyon	10	10	1.00	9	9	1.00
Black Butte	13	13	1.00	12	7	0.58
Imnaha	18	17	0.94	7	7	1.00
Lostine	33	32	0.97	14	13	0.93
Lower Hells Canyon	18	18	1.00	4	4	N/A
Mountain View	22	20	0.93	8	8	1.00
Muir Creek	3	3	N/A	1	1	N/A
Myers Creek/UHCID	3	3	N/A	1	1	N/A
Redbird	50	50	1.00	25	24	0.96
Saddle Creek	6	6	0.83	3	1	N/A
Tucannon	5	5	1.00	2	2	N/A
Wenaha	28	27	0.91	11	10	0.91
	0	0		0	0	
Total	230	222	0.97	100	89	0.89

We detected Movi in one Hells Canyon population (Lostine) in 2022. As of 2021, no females from the Lostine population were known to be Movi carriers and the one lamb tested was negative. Lamb recruitment was also improving, but Movi was detected in two of three adult males via testing. To further investigate infection in males, the males that tested positive in 2021 and an additional seven other males (total of eight adults and two yearlings) were tested in 2022. All individuals tested were negative for PCR (one male was indeterminate on the first swab and negative on the second swab submitted to WADDL). Five adult females were also tested; four had never been tested before, and all five tested negative for PCR (Table 10). However, Movi infection was detected in a lamb from the Lostine population, and antibodies to Movi were detected in 3 of 8 adult males; two males that were positive for infection in 2021 and an adult male that had not previously been tested (Table 10). Three of five females were also positive for antibodies (Table 10). All detections were in adult females that had not previously been tested. The only yearling tested for antibodies was positive (Table 10). Lamb survival was low in 2022 with an estimated 6 lambs surviving to 11 months, resulting in an estimated lamb:ewe ratio of 0.17 lambs per ewe.

Table 10. Summary of targeted *Mycoplasma ovipneumoniae* (Movi) testing in the Lostine, Oregon bighorn sheep population December 2022–April 2023.

Age class	<i>n</i>	PCR positive	Seropositive
Adult	13	0 (0%) ^a	6 (46%)
Yearling	2	0 (0%)	1 (100%) ^a
Lamb	1	1 (100%)	1 (100%)
Total	16	1	8 (53%)

^a serum was only collected from one of the yearlings tested.

Population Estimation Methods – We did not explore new approaches to population estimation for bighorn sheep during the past year. Estimating bighorn sheep demographics in an accurate and precise manner remains a challenge, and we continue to use the best available science and test new approaches as they become available.

Habitat, Nutrition, Movements, and Demographics – We continued our collaboration with the University of Idaho and University of Wyoming on investigations of bighorn sheep habitat, nutrition, movements, and demographics. In 2019 in collaboration with the Washington Department of Fish and Wildlife, we added a low-elevation study area containing the Asotin Creek, Washington herd from within the Hells Canyon metapopulation.

The University of Idaho, in collaboration with the University of Wyoming, completed 135 vegetation composition plots during the summers of 2021 and 2022, which resulted in >2,000

biomass samples and >1,500 forage quality samples from Asotin Creek and the Wind River Range near Dubois, Wyoming. All 2021 samples have been processed for crude protein, digestibility, and tannins. Samples that were collected during 2022 have been submitted to various labs and are nearly complete. In combination with the data collected during a previous graduate project from 2018–2019, we have completed the initial stages of analysis to estimate biomass of forage that meets energetic and protein requirements for lactating sheep (i.e., ‘usable biomass’) within Asotin Creek, Lost River Range, East Fork, and Owyhee River Canyon (Figure 14). Usable biomass generally declined as summer progressed, and by August, usable biomass declined to nearly zero across all study areas. The decline in usable biomass was especially pronounced in Asotin Creek after the Lick Creek Fire in July 2021, wherein usable biomass declined to zero a month earlier than other study areas. For our next steps, we are currently working on 1) predicting spatiotemporal variation in usable biomass within each study area, and 2) linking variation in usable biomass to movement, behavior, and fitness of bighorn sheep across the study areas.

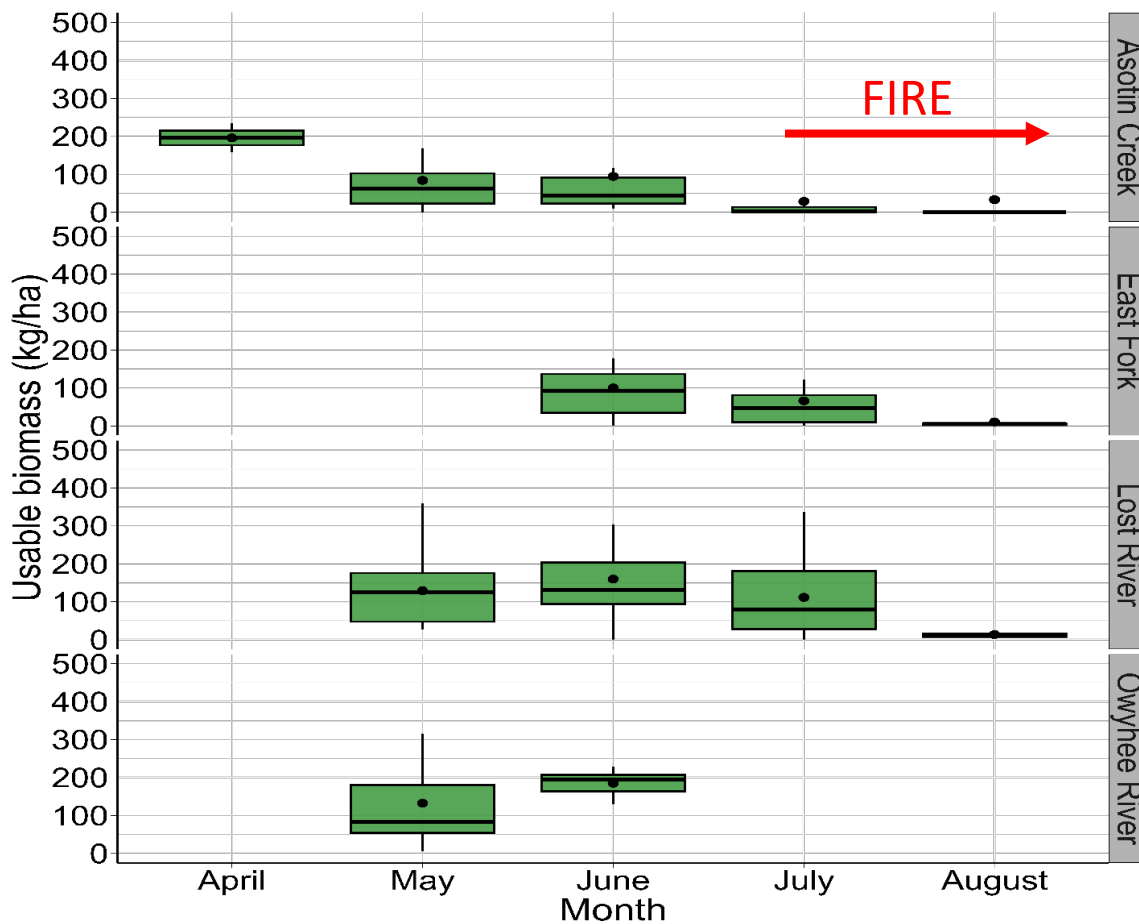


Figure 14. Estimated usable biomass from sampled transect locations during each month in Asotin Creek, 2021, and East Fork, Lost River, and Owyhee River Canyon 2018–2019. No data for a month indicates that transects were not sampled during that month. The red arrow indicates usable biomass estimates after the Lick Creek Fire in Asotin Creek that occurred on July 7, 2021.

We continued to monitor lambs that were captured during May and June of 2022 in Asotin Creek. We captured 14 live lambs and documented 1 stillborn. Most lambs were born between early to mid-May, but we captured a female lamb that was born on October 10, 2022 – over five months after peak parturition. The lamb was born a normal weight and survived to weaning—she is still alive currently. The late parturition date suggests that the dam was bred sometime in May of 2022, but the cause of the late conception is unclear. All captured lambs survived to weaning, and seven females and two males were still wearing collars at one year of age; however, five remaining lambs were censored before 1-year-of-age due to collars dropping off.

Two adult ewe mortalities occurred after July 2022, one attributed to meningoencephalitis, likely due to a bacterial infection, and one to unknown causes. Additionally, one female was censored in December 2022 due to collar drop off. During fall 2022, we attempted to re-capture all marked females. We did not attempt to replace mortalities because fall 2022 marked the end of the nutrition study.

Females that did not successfully recruit a lamb over the summer of 2022 were in better condition than females that did successfully recruit a lamb. Median ingesta-free body fat at capture for females that recruited a lamb was 12% (range 9–14%) and was 16% (range 15–17%) for females that did not recruit. Females that recruited a lamb over the summer in 2022 were in similar condition to females that recruited a lamb in 2019 and 2020, but in much better condition than females who recruited a lamb in 2021. Ewes were in relatively poor condition after the extreme drought and subsequent wildfire in the summer of 2021, however, the spring of 2022 was marked with record-breaking moisture which increased forage quality, and ultimately, improved nutritional condition during autumn 2022 (Figure 15).

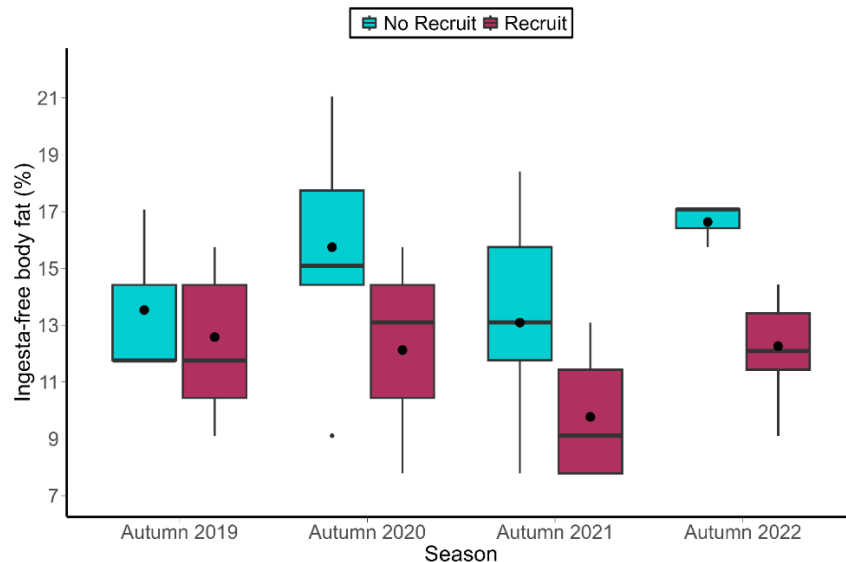


Figure 15. Fall estimates of percent ingesta-free body fat at capture for female bighorn sheep who were successful (teal) and unsuccessful (purple) at recruiting a lamb in Asotin Creek 2019–2021. Boxplots represent five number summary (i.e., minimum, 25th percentile, median, 75th percentile, maximum) and black dots represent population mean.

Genetic Diversity, Ancestry, and Connectivity – Two manuscripts are in progress on 1) genetic connectivity and diversity in Idaho native sheep and 2) genetic ancestry and diversity in reintroduced Rocky Mountain bighorn sheep populations in Idaho. These studies are being conducted in collaboration with the University of Idaho and University of Montana.

Investigation 5 – Moose Study

Monitoring Survival and Cause-specific Mortality – We monitored all surviving adult female moose that were fitted with collars during 2020 and 2021 ($n = 60$) during this reporting period. About half of the collared moose were located in the same study areas as the ongoing predator-prey research (described under the White-tailed Deer, Elk, Black Bear, Mountain Lion, and Wolf Projects) in GMUs 1, 6, and 10A (Table 11), while the remainder were spread across other moose populations in differing habitats. This sampling design allows us to both 1) fully integrate moose into the predator-prey investigations of north Idaho and 2) begin to assess vital rates and causes of mortality for moose in diverse habitat types across the Idaho.

We monitored collared moose to document survival, determine cause-specific mortality, and conduct monthly calf-at-heel surveys to assess summer calf survival and female body condition. A total of 13 collared moose died during the monitoring period. Known causes of death included vehicle collision (2 in GMU 1, 1 in GMU 78) and train collision (1 in GMU 1). Samples collected from carcasses of the 9 other collared mortalities are being analyzed to determine cause of death.

Table 11. Game management unit (GMU) of capture locations for adult female moose monitored during 2020 and 2021 ($n = 60$), Idaho.

GMU	Collared Moose	GMU	Collared Moose
1	15	64	1
6	7	66	5
8	1	67	1
8A	5	69	2
10A	3	71	2
51	1	74	1
54	2	75	1
55	1	76	2
60	1	78	4
60A	5		

Beginning in December 2022 we continued our investigation of moose mortality by capturing and monitoring 74 moose calves in multiple GMUs in the Panhandle, Clearwater, Southeast, and Upper Snake Regions (Table 12). A total of 12 collared moose calves died during the monitoring period. Known causes of death included auto accident ($n = 2$), heavy parasite infection ($n = 3$), lion predation ($n = 1$), malnutrition ($n = 4$), and unknown cause ($n = 1$).

Table 12. Game management unit (GMU) of capture locations for moose calves monitored during this reporting period ($n = 60$), Idaho.

GMU	Collared Calves	GMU	Collared Calves
1	14	71	3
4	2	72	1
6	12	73	2
8	2	75	4
60	2	76	3
64	1	78	2
65	3	10A	6
66	3	60A	4
69	3	8A	5
70	2		

Abundance Modeling from Trail Camera Data - In GMUs 1, 6, and 10A, we continue to deploy and maintain 750 cameras (see Alternative Monitoring Methods in the Mule Deer Project) to estimate summer abundances of multiple species, including moose. Images have been collected and processed and preliminary moose abundance estimates for summer 2021 were detailed during the last reporting period. We have processed images collected from summer 2022 and will collect images from summer 2023 in fall 2023. Abundance estimates for summer 2022 are still pending, and we are continuing work to define our methodologies for camera-based population estimation.

Investigation 6 – Pronghorn Study

We assisted Survey and Inventory project staff in capturing and collaring 152 adult and yearling pronghorn across southern Idaho during capture efforts between July 2020 and June 2022, primarily in mountain valley habitats that were underrepresented in IDFG’s prior pronghorn monitoring efforts. We supplemented the sample of monitored pronghorn with additional captures between July 2022 and June 2023, adding another 20 collared pronghorn (Table 13). We monitored the movements and survival of all collared pronghorn since capture.

Table 13. Adult or yearling pronghorn collared between July 2022 and June 2023, Idaho.

Sex	IDFG Region	
	Magic Valley	Upper Snake
Male	1	3
Female	6	10
Total	7	13

A total of 70 collared pronghorn died from non-capture related causes during July 2020–July 2023 monitoring. Causes of death included predation by mountain lions ($n = 11$), coyotes ($n = 15$), and unknown predator species ($n = 6$); harvest (legal = 12, illegal = 2); disease ($n = 1$); accidents ($n = 5$); and unknown causes ($n = 18$).

We also developed and evaluated a new method for identifying stopovers that ungulates use along migration routes (see the *Seasonal Range and Migration Modeling* section of the Mule Deer Study). For four herds that consisted of 146 tracked migrations of individual collared pronghorn, we found that when compared to the methods proposed by Sawyer and Kauffman (2011), false positives (prior method suggested additional stopovers) were found to occur at a rate of 48%. False negatives (prior method failed to identify stopovers) occurred at a much higher rate of 27%. At the population level, false positives and false negatives occurred at 60% and 30%, respectively. The methods and associated findings were presented at the WAFWA Pronghorn workshop in August 2022 in Deadwood, South Dakota. The analyses identifying mule deer, elk, and pronghorn stopovers are being prepared for publication as a peer-reviewed manuscript.

We also estimated and delineated the pronghorn antelope migration route for the Shotgun Valley in south-eastern Idaho. This database has been added to IDFG’s existing ungulate migration database and published in USGS’s *Ungulate Migration of the Western United States, Volume 3* (Kauffman et al. 2022).

Investigation 7 – Mountain Goat Study

No progress was made on this investigation during the reporting period because capture time was limited due to extreme weather and other scheduled captures took precedence. In conjunction with Survey and Inventory project staff, we plan to pursue the capture and collaring of up to 15 mountain goats in the next reporting period.

Investigation 8 – Gray Wolf Study

Estimating Wolf Abundance and Distribution - We retrieved (fall 2022) and redeployed (spring 2023) 207 wolf occupancy cameras (set to take motion-triggered photos with one camera per 686-km² grid cell) and 566 abundance cameras (set to take motion- and time-triggered photos and placed within 32.9-km² sub-cells nested within each randomly selected occupancy grid cell) during the reporting period. When possible, we positioned all cameras in the same locations as previous years. Consistent with prior surveys, we used occupancy estimates from 2016–2018 to stratify statewide occupancy cells into high, medium, or low strata. We then used generalized random tessellation sampling to select 37 occupancy grid cells across the state for abundance estimation. We selected occupancy grid cells so that 50% of effort went to the low occupancy stratum, 30% to the medium occupancy stratum, and 20% to high occupancy stratum. Each selected occupancy grid cell was then split into 16 sub-cells and an abundance camera was placed in each sub-cell. Within the selected occupancy grid cells and abundance sub-cells, cameras were placed in locations consistent with previously developed occupancy sampling protocols that relied on predicting and sampling wolf rendezvous site habitat (i.e., denning and pup-rearing habitat). Some cameras contributed data to both the occupancy and abundance datasets.

A total of 10.7 million photos were taken by all cameras combined during summer of 2022 (abundance and occupancy). We utilized an AI image processing tool developed by Microsoft AI for Earth (“the MegaDetector) that gives us a likelihood that each picture contains an animal or not. The MegaDetector has proven very accurate in testing to date and allows us to avoid manually reviewing about 95% of time-triggered photos. We have also worked with Microsoft to develop and test a classification system that identifies and pre-labels species in photos and further reduces time spent manually reviewing images. After processing all photos using both the MegaDetector and manual screening, we identified 5,294 photos containing wolves; with wolf detections at 180 out of 712 sampled locations.

We used a space-to-event analysis to estimate the number of wolves by stratum (Moeller et al. 2018). We limited the analysis period to July 1, 2022–August 31, 2022 to provide a period of relatively consistent wolf numbers (once young of year are highly mobile and prior to the when the majority of harvest occurs). To estimate abundance, we extrapolated the estimated mean wolf density for each stratum (wolves per square meter) to the area of predicted rendezvous site habitat within each stratum, after areas of water and human development were removed. The 2022 estimated statewide wolf abundance was 1,323 (95% CI = 997–1756; Table 14).

Table 14. Wolf abundance estimates (\hat{N}) and 95% confidence intervals (lower confidence bound = lcb – UCL) across three strata from camera data, 2022, Idaho. Note: the area represents the total stratum area, not the predicted high-use, wolf rendezvous habitat only.

Stratum	Area (km²)	\hat{N}	LCL	UCL	Density (per 1000 km²)
Low	36,358	315	240	415	8.6
Medium	37,044	494	365	669	17.8
High	37,044	514	393	672	13.9
Total	110,446	1,323	998	1756	12.0

We also used a dynamic occupancy model to assess initial occupancy, local immigration (instances where a cell transitions from unoccupied to occupied), local emigration (instances where a cell transitions from occupied to unoccupied), and detection probability for wolves across the state (Mackenzie et al. 2006). The results of this analysis indicated wolf occupancy, emigration, and immigration are most strongly influenced by habitat and neighboring cell occupancy. We further explored occupancy with single-season occupancy models which revealed a complex relationship between wolf harvest and wolf occupancy. At lower levels of harvest, occupancy was positively related to harvest. This is likely because harvest will tend to be greatest in areas where wolves are more abundant. At higher harvest levels, however, we saw some evidence that occupancy may be negatively related to harvest. These analyses were published in Ausband et al. (2023).

In GMUs 1, 6, and 10A, we deployed and maintained 750 cameras (see *Alternative Monitoring Methods* section of Mule Deer Study) to estimate summer abundance of multiple species, including wolves. We collected data from these cameras in fall 2021 and generated preliminary summer wolf abundance estimates for each of those GMUs. We did not capture a sufficient number of images to estimate wolf abundance using the randomly placed cameras but did generate an estimate using images from cameras placed on roads and trails in a space-to-event model. We estimated 65 (95% CI 30–140), 59 (95% CI 36–95), and 75 (95% CI 44–126) wolves in GMUs 1, 6, and 10A, respectively, which was reported in the previous reporting period. We are currently working on validating those estimates. Images from 2022 are still undergoing review and error checking, when complete, we will use images to estimate wolf density in each study GMU.

We also are currently exploring alternative approaches to estimating wolf abundance in Idaho. Hunters who harvest wolves in Idaho must report information on the date and location of the harvest, the sex of the wolf, and provide a tooth that can be used for aging and genetic analysis. This information, specifically data on age-at-harvest, can be incorporated into a class of demographic models known as statistical population reconstruction (SPR) models to estimate abundance, survival, and recruitment. While SPR models come in many shapes and sizes, all require the age-at-harvest data and hunter effort be supplemented with auxiliary information,

such as independent estimates of survival or abundance (Gove et al. 2002). However, these auxiliary estimates are not needed for every year during which demographic estimates are being made. We used the software program PopRecon 2.0 (Clawson et al. 2017) to assess the efficacy of SPR to estimate wolf abundance in Idaho.

Hunter effort is an important parameter in SPR models but is challenging to quantify for wolf hunters because they consist of both hunters that harvest wolves opportunistically as they pursue other species and hunters that are intentionally hunting and harvesting wolves. Thus, we derived an index of hunter effort by calculating the annual average number of trap nights over a 9-year period (2012–2020). We then restricted our data set to age-at-harvest to trapped wolves. We estimated annual probability of harvest due to trapping using data on wolves collared during 2012–2016. Finally, we supplemented our SPR model with a wolf abundance estimate for 2019 generated from our statewide wolf abundance camera work. Initial results demonstrated that the camera-based abundance estimate from 2019 fell within the 95% confidence interval of our SPR estimate. Although these results are promising, we are exploring ways to include additional data sources into the SPR framework with the goal of reducing monitoring costs and increasing precision.

Predator/Prey and Predator/Predator Relationships – We are supporting a postdoctoral researcher at the University of Idaho to understand the relationships among large carnivore species in northern Idaho. Using camera data collected in GMUs 1, 6, and 10A (see *Alternative Monitoring Methods* in Mule Deer Study), we first examined spatial relationships among black bears, wolves, mountain lions, coyotes, and bobcats. We evaluated spatial relationships between each pair of predator species at three temporal scales (over a season [June–August], from week-to-week, and as the time until detection after detecting a competitor) using multispecies occupancy models and generalized linear models. There was minimal evidence to suggest negative interactions between predator species with the exception of coyotes avoiding areas containing bobcats where high snowshoe hare densities existed (Figure 16). The effect was not present in low-density snowshoe hare areas, which suggested that bobcats, being superior hunters of snowshoe hares, might competitively exclude coyotes from areas with high hare densities. At the weekly scale, we observed several positive predator-predator interactions (Figure 17), which suggested similar habitat selection among species or potentially some degree of facilitation (i.e., scavenging opportunities for a subordinate predator). Overall, abiotic (e.g., elevation) and biotic (e.g., prey and vegetation) factors were a greater influence than predator-predator interactions (Figure 18). This work is being prepared for submission to *Ecological Monographs*. In the reporting period, we plan to shift from examining spatial interactions among predators to determining if certain predator species negatively influence the survival or productivity of competing predators.

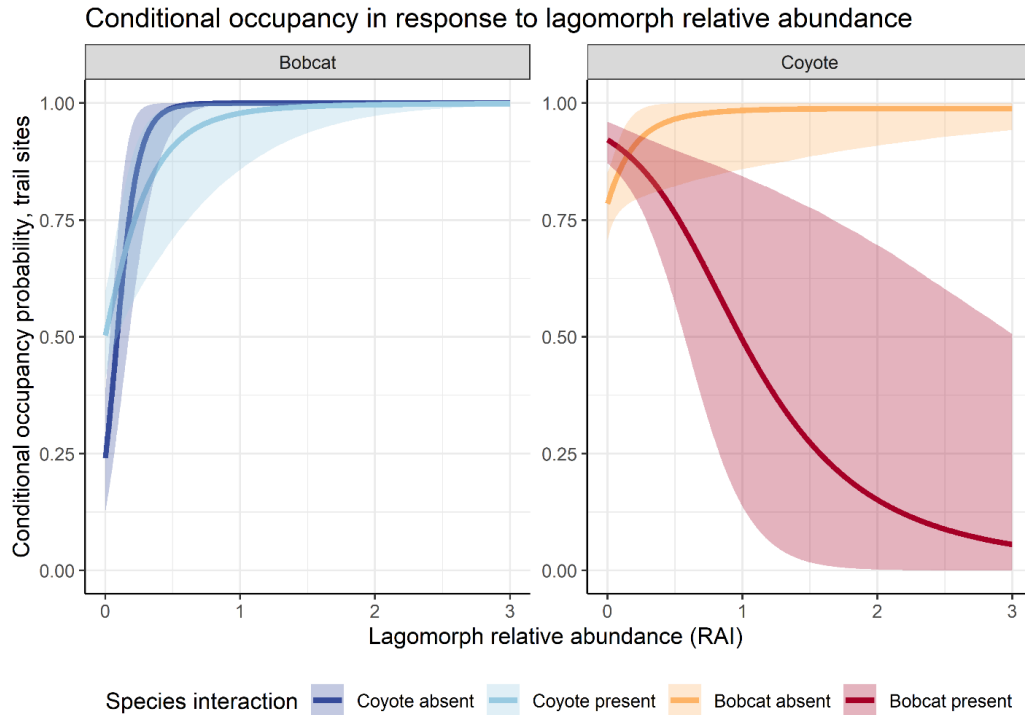


Figure 16. Influence of relative abundance index (RAI) of lagomorphs on the predicted probability of use for coyotes and bobcats, conditional on whether the other predator was present or absent from sites in northern Idaho, USA, summer 2020–2021.

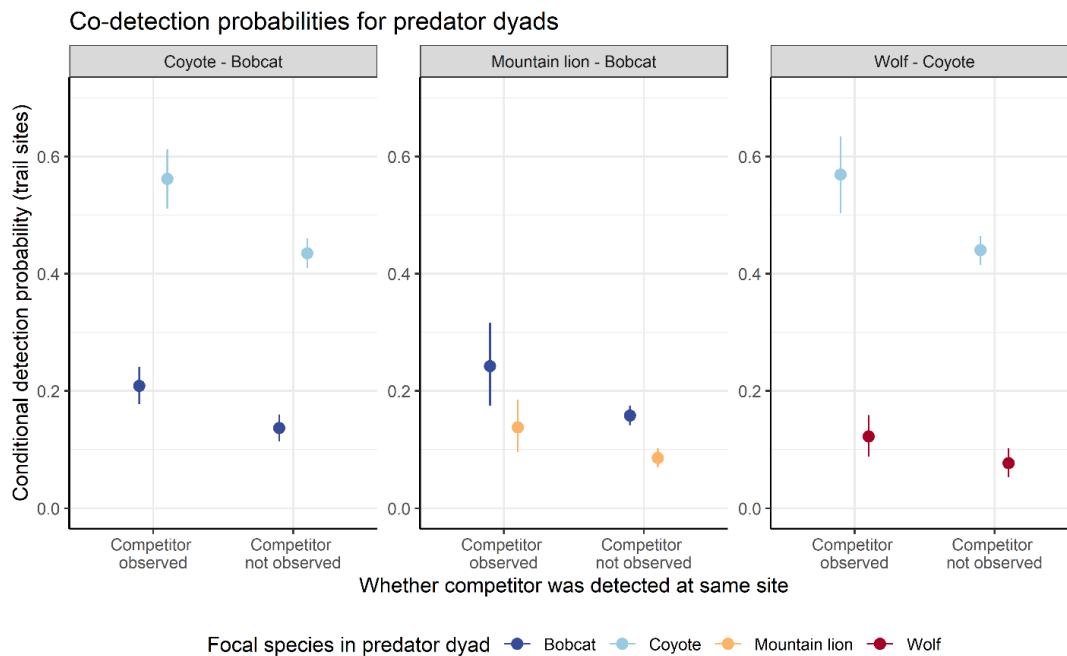


Figure 17. Mean detection probability for bobcats, coyotes, mountain lions, and wolves, conditional on whether a competitor was also observed at the same site during a 1-week sampling occasion in northern Idaho, USA, summer 2020–2021.

Species-specific marginal occupancy across elevation, percent forest cover, and prey diversity gradients

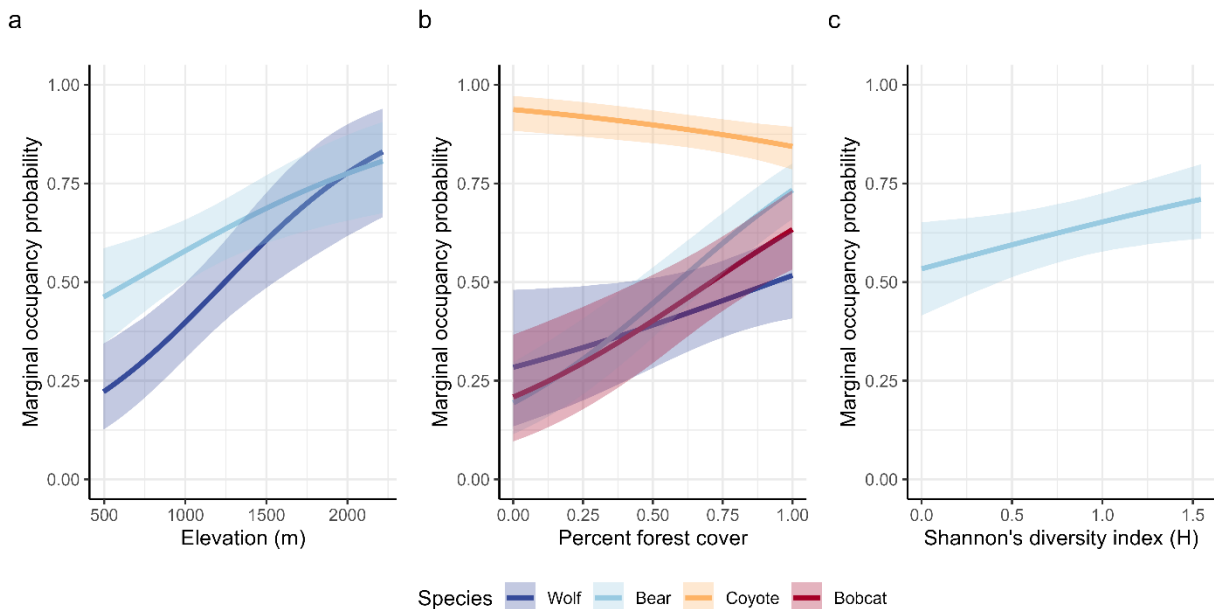


Figure 18. Effect of (a) elevation, (b) percent forest cover, and (c) prey diversity (Shannon's diversity index) on the predicted marginal probability of site use for black bears, bobcats, coyotes, and wolves at trail sites in northern Idaho, 2020–2021. The posterior mean for each species and covariate relationship are represented by the dark line and the 95% credible intervals (CRI) are represented by the partly transparent ribbons.

We are also contracting with Rogue Detection Teams, LLC ([Rogue Detection Teams \(roguedogs.org\)](https://roguedogs.org)) to collect predator scats in GMUs 1, 6, and 10A to better understand the relationships among predator and prey species in northern Idaho. This effort is in support of a PhD project at the University of Montana. Trained scat detecting dogs and handlers are targeting scats from black bears, wolves, mountain lions, coyotes, and bobcats. Scats are then dried and sent to a lab at Oregon State University for metabarcoding to identify the species of prey DNA contained in each scat. Surveys were conducted in winter 2023 and spring 2023 (Table 15) and three additional surveys are scheduled for the next reporting period. Genetic analysis is yet to be completed. Understanding the contribution of prey species to the diet of each predator and the seasonal variation will assist in teasing apart some of the complexity of multi-predator, multi-prey systems.

Table 15. The number of scats collected in GMUs 1, 6, and 10A in Winter and spring 2023 and their putative species identification.

	GMU	GMU	GMU			GMU	GMU	GMU	
Winter 2023	1	6	10A	Total	Spring 2023	1	6	10A	Total
Bobcat	21	22	9	52	Bobcat	44	56	32	132
Coyote	38	37	20	95	Coyote	48	68	72	188
Mountain lion	12	12	5	29	Mountain lion	15	34	11	60
Wolf	18	8	25	51	Wolf	18	14	30	62
Bear	0	0	0	0	Bear	43	19	2	64

Investigation 9 – Mountain Lion Study

In GMUs 1, 6, and 10A, we deployed and maintained 750 cameras (see *Alternative Monitoring Methods* within the Mule Deer Study) to estimate abundance of multiple species, including mountain lions. We collected data from these cameras in fall 2021 and have generated preliminary summer mountain lion abundance estimates for each of those GMUs. We did not capture a sufficient number of pictures to estimate mountain lion abundance using the randomly placed cameras but did generate an estimate using the cameras that were placed on roads and trails with a space-to-event model. We estimated 127 (95% CI 73–221), 86 (95% CI 58–129), and 59 (95% CI 33–106) mountain lions in GMUs 1, 6, and 10A, respectively, which was reported in the prior reporting period. We are still assessing and refining those estimates. We collected data from these cameras again in the fall of 2022 but have not completed the analysis and will again retrieve images from these cameras in fall 2023.

We also assisted Survey and Inventory project staff in the design and deployment of a camera array in the Bannock mule deer DAU (GMUs 56, 57, 70, 73, and 73A) in fall 2021. Data from winter 2021–2022 generated a preliminary estimate of 172.0 mountain lions in the study area using a space-to-event model with 91 functioning randomly placed cameras (95% CI 33.6–879.3). The large confidence interval indicates that an insufficient number of cameras were deployed to estimate mountain lions at this density. We plan to further explore ways to generate more accurate mountain lion estimates. We continue to collect and age teeth from harvested mountain lions, which could be used in an SPR model as was presented in the *Estimating Wolf Abundance and Distribution* section within the Gray Wolf Study, but to date, we have not developed a mountain lion SPR model.

We have shifted our approach to monitoring mountain lions and their relationships with other predators and prey from collar-based to camera-based efforts. Therefore, we did not attempt to capture and collar mountain lions during this reporting period. We are currently supporting a postdoctoral researcher at the University of Idaho to examine predator-predator relationships, including relationships between mountain lions and other predators, and are working with a graduate student at the University of Montana and contracting Roque Detection Dogs, LLC

([Rogue Detection Teams \(roguedogs.org\)](http://roguedogs.org)) and an Oregon State University Lab to collect and genetically test mountain lion scats to examine seasonal changes in mountain lion prey. Details for both projects are located in the *Predator/Prey and Predator/Predator Relationships* section of the Gray Wolf Study.

Investigation 10 – Black Bear Study

In GMUs 1, 6, and 10A, we deployed and maintained 750 cameras (see *Alternative Monitoring Methods* in Mule Deer Study) to estimate abundance of multiple species, including black bears. We collected data from these cameras in fall 2021 and 2022 and generated preliminary summer black bear abundance estimates for each of those GMUs. We did not capture a sufficient number of pictures to estimate black bear abundance using the randomly placed cameras but did generate an estimate using the cameras that were placed on roads and trails with a space-to-event model. Using data from summer 2021, we estimated 2,473 (95% CI 1,746–3,503), 837 (95% CI 593–1,182), and 520 (95% CI 305–886) black bears in GMUs 1, 6, and 10A, respectively. We are continuing to assess and refine those estimates. We collected data from these cameras again in the fall of 2022 but have not completed the analysis and will again retrieve images from these cameras in fall 2023.

We continue to collect and age teeth from harvested black bears, which could be used in an SPR model as was presented in the *Estimating Wolf Abundance and Distribution* section within the Gray Wolf Study, but to date, we have not developed a black bear SPR model. We also are currently supporting a postdoctoral researcher at the University of Idaho to examine predator-predator relationships, including relationships between black bears and other predators, and are working with a graduate student at the University of Montana and contracting Rogue Detection Dogs, LLC ([Rogue Detection Teams \(roguedogs.org\)](http://roguedogs.org)) and an Oregon State University Lab to collect and genetically test black bear scats to examine seasonal changes in mountain lion prey. Details for both projects are located in the *Predator/Prey and Predator/Predator Relationships* section of the Gray Wolf Study.

Investigation 11 – Greater Sage-grouse Study

Effect of Livestock Grazing – This long-term, landscape-scale project has been ongoing for nine years and encompasses five study areas. To date, we have monitored the survival, habitat selection, and reproductive effort and success of 1,260 female greater sage-grouse (Table 16). Female survival during the breeding season varied across sites in 2022 and has varied from 60% to 85% during 2014–2022 (Figure 19). We have monitored the success of 979 nests during the study to date (Figure 20; 176 nests monitored in 2022).

Grazing schedules for treatment pastures within each study area follow a before-after control-impact design (Figure 21). The 2 years of pre-treatment monitoring allow us to determine where sage-grouse nests are most likely to be located and allow us to measure survival and reproductive parameters at the site under the current management conditions. The study areas are divided into four pastures and four years of treatments are implemented in each pasture; with alternate years of spring grazing for two pastures, no livestock grazing at all for one pasture, and alternating spring/fall grazing for one pasture.

Table 16. Adult and yearling female greater sage-grouse captured and collared for the sage-grouse and grazing project, Idaho, 2014–2022.

Age	2014	2015	2016	2017	2018	2019	2020	2021	2022
Adult	52	57	82	76	90	116	110	159	78
Yearling	40	51	38	55	33	79	39	47	58
Total	92	108	120	131	123	195	149	206	136

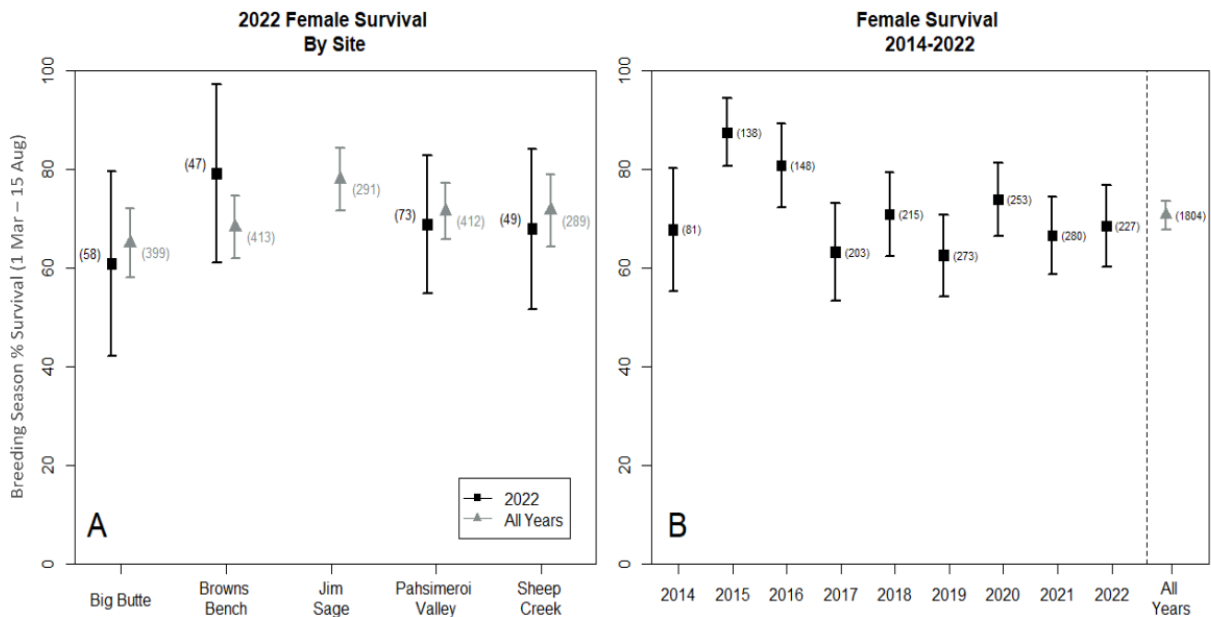


Figure 19. Survival estimates and 95% confidence intervals of female sage-grouse at 5 study sites in 2022 (A) and by year for all study sites pooled (B) during our monitoring period (1 Mar–15 Aug). Number to the right of each estimate represents the number of hens whose encounter histories contributed to the estimate.

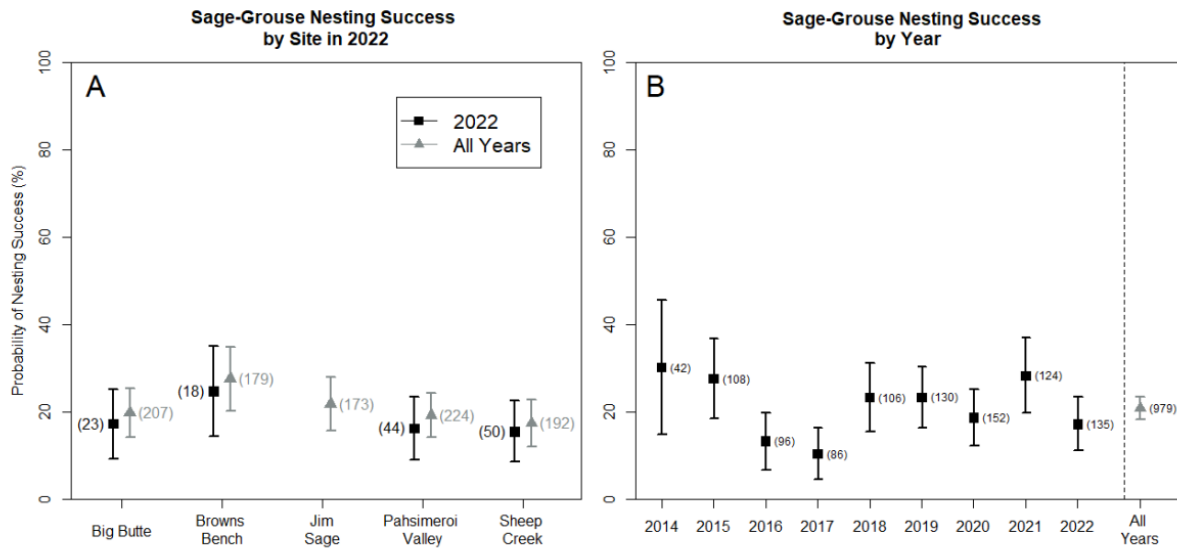


Figure 20. Probability of nest survival and 95% confidence intervals A) for each study site in 2022 B) and for each year (combined across all study sites), 2014–2022. Estimates were extrapolated from daily nest survival to estimate the overall nest survival across the laying and incubation period (37 days).

Treatment	Year 1	Year 2	Implement Grazing Treatments	Year 3	Year 4	Year 5	Year 6
Spring Odd Years	Current grazing	Current grazing		Spring Grazing	No Grazing	Spring Grazing	No Grazing
Spring Even Years	Current grazing	Current grazing		No Grazing	Spring Grazing	No Grazing	Spring Grazing
No Grazing	Current grazing	Current grazing		No Grazing	No Grazing	No Grazing	No Grazing
Spring and Fall	Current grazing	Current grazing		Spring Grazing	Fall Grazing	Spring Grazing	Fall Grazing

Figure 21. Monitoring and treatment schedule used to evaluate effects of cattle grazing on sage-grouse demographic traits and habitat features within 4 treatment pasture types at each southern Idaho project study area.

We deployed and maintained over 42 km of temporary electric fence (solar powered) in 2022 to aid in utilization and livestock distribution and to allow permittees to continue their regular grazing schedules on portions of pastures not used by nesting sage-grouse. We used visual estimates of forage utilization and measurements of vegetation height along transects to quantify forage utilization in each study pasture at the end of each growing season. We also sampled vegetation at nest sites and random plots within our treatment and control pastures. Analyses of those data are ongoing.

Sage-grouse Ecology in High-elevation Sagebrush Habitats – Sage-grouse inhabiting mountain foothill, higher-elevation habitats (i.e., dominated by mountain big sagebrush and/or low sagebrush above 1,500 m elevation; hereafter high-elevation sagebrush) may or may not interact with their habitat similarly to sage-grouse inhabiting the more-studied, lower-elevation habitats of southern Idaho (i.e., dominated by Wyoming big sagebrush). In association with researchers at the University of Idaho, we used survival, reproduction, location, and vegetation data from GPS-marked sage-grouse to model the relationship between sage-grouse fitness and habitat in these unique landscapes. This examination was completed concurrently with analyses completed under the *Effects of Wildfire on Habitat Selection and Demographics* section and was jointly described in the prior reporting period. Work from both sections was published during the current reporting period (Stevens et al. 2023).

Effects of Wildfire on Habitat Selection and Demographics – During late July–early August of 2018, the Grassy Ridge fire burned approximately 99,000 acres of the Sand Creek desert, one of the study areas in the previously described *Sage-grouse Ecology in High-elevation Sagebrush Habitats* section. We used pre- and post-fire sage-grouse data with regression-based analyses and information theoretic model selection approaches to compare pre- and post-fire habitat selection and demographics. This examination was completed concurrently with analyses completed under the *Sage-grouse Ecology in High-elevation Sagebrush Habitats* section and was jointly described in the prior reporting period. Work from both sections was published during the current reporting period (Stevens et al. 2023).

Investigation 12 – Effects of Agriculture Landscape Change on Wildlife Populations

We continued the development of approaches to estimate the intensity of agriculture use in southeastern Idaho. In the past, we acquired annual maps of active agriculture within Idaho from 2008–2021. As part of these efforts, we used multi-temporal NDVI databases developed with terraPulse (<http://www.terrapulse.com>) for the purpose of estimating how many crop cycles occurred within specific agricultural fields. From NDVI annual trajectories, where NDVI is measured on a daily increment, we estimated the number of crop rotations that had occurred within each year. Initially, we thought that an individual field maintained high spatial fidelity, meaning a field’s boundaries would be maintained through time, but instead, observed that field boundaries often changed through time. This finding suggested that we needed a finer-scale resolution to estimate changes in crop field boundaries. To meet spatiotemporal needs, we pursued the development of algorithms that tracked crop rotations on a per pixel basis (30m). The algorithms identified the growth-harvest-growth cycles by tracking the rate of NDVI increases and identified when the NDVI trajectory changed abruptly. By identifying the number of NDVI trajectory changes per annum, we anticipated being able to accurately estimate the number of crop rotations per year for a given field. We identified over 6,000 fields within southeastern Idaho and performed a multi-annual analysis across subsets of pixels within each of

these fields. Preliminary analyses suggested that we need to adapt our methodology as the results failed to consistently identify a whole number (e.g., 1, 2, 3, etc.) of crop rotations. We will continue to develop our approach to estimating crop rotations as an index agricultural intensity with the goal of quantifying the effects of increasing agricultural intensity on species, such as Columbia sharp-tailed grouse, pronghorn antelope, and mule deer.

Literature Cited

- Ausband, D. E., Thompson, S. J., Oates, B. A., Roberts, S. B., Hurley, M. A., & Mumma, M. A. (2023). Examining dynamic occupancy of gray wolves in Idaho after a decade of managed harvest. *The Journal of Wildlife Management* e22453. <https://doi.org/10.1002/jwmg.22453>
- Bunnefeld, N., Börger, L., van Moorter, B., Rolandsen, C.M., Dettki, H., Solberg, E.J. and Ericsson, G. (2011), A model-driven approach to quantify migration patterns: individual, regional and yearly differences. *Journal of Animal Ecology* 80:466–476. <https://doi.org/10.1111/j.1365-2656.2010.01776.x>
- Clark, T.J., J.S. Horne, M. Hebblewhite, and A.D. Luis. Stochastic predation exposes prey to predator pits and local extinction. *Oikos* 130:300–309. <https://doi.org/10.1111/oik.07381>
- Clawson, M.V., J.R. Skalski, J.M. Lady, C.A. Hagen, J.J. Millspaugh, D. Budeau, and J.P. Sevenson. 2017. Performing Statistical Population Reconstruction Using Program PopRecon 2.0. *Wildlife Society Bulletin* 41:581–589. <https://doi.org/10.1002/wsb.790>
- Fisk, E.A., E.F. Cassirer, K.S. Huggler, A.P. Pessier, *et al.* 2023. Abortion And Neonatal Mortality due to *Toxoplasma Gondii* in Bighorn Sheep (*Ovis Canadensis*). *Journal of Wildlife Diseases* 59:37–48. <https://doi.org/10.7589/JWD-D-22-00057>
- Gove, N. E., J. R. Skalski, P. Zager, and R. Townsend. 2002. Statistical models for population reconstruction using age-at-harvest data. *Journal of Wildlife Management* 66:310–320. <https://doi.org/10.2307/3803163>
- Kauffman, M., Lowrey, B., Berg, J., Bergen, S., Brimeyer, D., Burke, P., Cufaude, T., Cain, J.W., III, Cole, J., Courtemanch, A., Cowardin, M., Cunningham, J., DeVivo, M., Diamond, J., Duvuvuei, O., Fattebert, J., Ennis, J., Finley, D., Fort, J., Fralick, G., Freeman, E., Gagnon, J., Garcia, J., Gelzer, E., Graham, M., Gray, J., Greenspan, E., Hall, E., Hendricks, C., Holland, A., Holmes, B., Huggler, K., Hurley, M., Jeffreys, E., Johnson, A., Knox, L., Krasnow, K., Lockyer, Z., Manninen, H., McDonald, M., McKee, J.L., Meacham, J., Merkle, J., Moore, B., Mong, T.W., Nielsen, C., Oates, B., Olsen, K., Olson, D., Olson, L., Pieron, M., Powell, J., Prince, A., Proffitt, K., Reddell, C., Riginos, C., Ritson, R., Robatcek, S., Roberts, S., Sawyer, H., Schroeder, C., Shapiro, J., Simpson, N., Sprague, S., Steingisser, A., Tatman, N., Turnock, B., Wallace, C., and Wolf, L., 2022, Ungulate migrations of the western United States, volume 3: U.S. Geological Survey Scientific Investigations Report 2022–5088. <https://doi.org/10.3133/sir20225088>

- Kauffman, M.K., Jakopak, J., Olson, L., Randall, J., Rozman, G., Berg, J., Bergen, S., Garcia, J., Greenspan, E., Hurley, M., and C. Schoeder. 2023. Migration. In J.R. Heffelfinger and P.R. Krausman (Eds.), *Ecology and Management of Black-tailed and Mule Deer of North America* (1st ed., pp. 383-394). CRC Press. DOI:10.1201/9781003354628
- MacKenzie, D. 2006. Modeling the probability of resource use: the effect of, and dealing with, detection a species imperfectly. *The Journal of Wildlife Management* 70:367–374. [https://doi.org/10.2193/0022-541X\(2006\)70\[367:MTPORU\]2.0.CO;2](https://doi.org/10.2193/0022-541X(2006)70[367:MTPORU]2.0.CO;2)
- Moeller, A.K., P.M. Lukacs, and J.S. Horne. 2018. Three novel methods to estimate abundance of unmarked animals using remote cameras. *Ecosphere* 9:e02331. <https://doi.org/10.1002/ecs2.2331>
- Sawyer, H. and Kauffman, M.J. 2011 Stopover ecology of a migratory ungulate. *Journal of Animal Ecology*, 80: 1078–1087. <https://doi.org/10.1111/j.1365-2656.2011.01845.x>
- Stevens, B.S., S.B. Roberts, C.J. Conway, and D.K. Englestead. 2023. Effects of large-scale disturbance on animal space-use: Functional responses by greater sage-grouse after megafire. *Ecology and Evolution* 13:e9933. <https://doi.org/10.1002/ece3.9933>
- van de Kerk, M., R.T. Larsen, D.D. Olson *et al.* 2021. Variation in movement patterns of mule deer: have we oversimplified migration? *Movement Ecology* 9:44. <https://doi.org/10.1186/s40462-021-00281-7>

Publications

- Ausband, D. E., Thompson, S. J., Oates, B. A., Roberts, S. B., Hurley, M. A., & Mumma, M. A. (2023). Examining dynamic occupancy of gray wolves in Idaho after a decade of managed harvest. *The Journal of Wildlife Management* e22453. <https://doi.org/10.1002/jwmg.22453>
- Fisk, E.A., E.F. Cassirer, K.S. Huggler, A.P. Pessier, *et al.* 2023. Abortion And Neonatal Mortality due to *Toxoplasma Gondii* in Bighorn Sheep (*Ovis Canadensis*). *Journal of Wildlife Diseases* 59:37–48. <https://doi.org/10.7589/JWD-D-22-00057>
- Kauffman, M., Lowrey, B., Berg, J., Bergen, S., Brimeyer, D., Burke, P., Cufaude, T., Cain, J.W., III, Cole, J., Courtemanch, A., Cowardin, M., Cunningham, J., DeVivo, M., Diamond, J., Duvuvuei, O., Fattebert, J., Ennis, J., Finley, D., Fort, J., Fralick, G., Freeman, E., Gagnon, J., Garcia, J., Gelzer, E., Graham, M., Gray, J., Greenspan, E., Hall, E., Hendricks, C., Holland, A., Holmes, B., Huggler, K., Hurley, M., Jeffreys, E., Johnson, A., Knox, L., Krasnow, K., Lockyer, Z., Manninen, H., McDonald, M., McKee, J.L., Meacham, J., Merkle, J., Moore, B., Mong, T.W., Nielsen, C., Oates, B., Olsen, K., Olson, D., Olson, L., Pieron, M., Powell, J., Prince, A., Proffitt, K., Reddell, C., Riginos, C., Ritson, R., Robatcek, S., Roberts, S., Sawyer, H., Schroeder, C., Shapiro, J., Simpson, N., Sprague, S., Steingisser, A., Tatman, N., Turnock, B., Wallace, C., and Wolf, L., 2022, *Ungulate migrations of the western United States, volume 3: U.S. Geological Survey Scientific Investigations Report 2022–5088*. <https://doi.org/10.3133/sir20225088>

Stevens, B.S., S.B. Roberts, C.J. Conway, and D.K. Englestead. 2023. Effects of large-scale disturbance on animal space-use: Functional responses by greater sage-grouse after megafire. *Ecology and Evolution* 13:e9933. <https://doi.org/10.1002/ece3.9933>

Name, title, phone number, and e-mail address of person compiling this report:

Matt Mumma
Wildlife Research Manager
matt.mumma@idfg.idaho.gov

FEDERAL AID IN WILDLIFE RESTORATION

The Federal Aid in Wildlife Restoration Program consists of funds from a 10% to 11% manufacturer's excise tax collected from the sale of handguns, sporting rifles, shotguns, ammunition, and archery equipment. The Federal Aid program then allots the funds back to states through a formula based on each state's geographic area and the number of paid hunting license holders in the state. The Idaho Department of Fish and Game uses the funds to help restore, conserve, manage, and enhance wild birds and mammals for the public benefit. These funds are also used to educate hunters to develop the skills, knowledge, and attitudes necessary to be responsible, ethical hunters. Seventy-five percent of the funds for this project are from Federal Aid. The other 25% comes from license-generated funds.

